Applications of Mathematics

Mária Lukáčová-Medviďová; Jitka Saibertová; Gerald G. Warnecke; Yousef Zahaykah

On evolution Galerkin methods for the Maxwell and the linearized Euler equations

Applications of Mathematics, Vol. 49 (2004), No. 5, 415–439

Persistent URL: `http://dml.cz/dmlcz/134577`

49 (2004) APPLICATIONS OF MATHEMATICS No. 5, 415–439

ON EVOLUTION GALERKIN METHODS FOR THE MAXWELL AND THE LINEARIZED EULER EQUATIONS*

Mária Lukáčová-Medviďová, Hamburg and Brno, Jitka Saibertová, Brno, Gerald Warnecke, Magdeburg, and Yousef Zahaykah, Magdeburg

(Received August 19, 2002, in revised version January 29, 2003)

Abstract. The subject of the paper is the derivation and analysis of evolution Galerkin schemes for the two dimensional Maxwell and linearized Euler equations. The aim is to construct a method which takes into account better the infinitely many directions of propagation of waves. To do this the initial function is evolved using the characteristic cone and then projected onto a finite element space. We derive the divergence-free property and estimate the dispersion relation as well. We present some numerical experiments for both the Maxwell and the linearized Euler equations.

Keywords: hyperbolic systems, wave equation, evolution Galerkin schemes, Maxwell equations, linearized Euler equations, divergence-free, vorticity, dispersion

MSC 2000:

1. Introduction

Evolution Galerkin methods, EG methods, were proposed to approximate the solution of evolutionary problems of first order hyperbolic systems. Ostkamp in [9] as well as Lukáčová, Morton and Warnecke in [4], [5] derived such schemes for the approximation of the solution of the wave equation system and the Euler equations of gas dynamics in two dimensions. In [11] the approximate evolution operator for the wave equation system in three space dimensions as well as other 2D EG schemes were derived.

* This research was supported under the DFG grant No. Wa 633/6-2 of Deutsche Forschungsgemeinschaft, by the grants no. 201/00/0557 and 201/03/0570 of the Grant Agency of the Czech Republic as well as by the Volkswagen Stiftung and DAAD Agencies.

It is well-known, see [4], [5], [8], [9], that the basic tool to derive the EG schemes is the general theory of bicharacteristics of linear hyperbolic systems. This theory is used to derive the system of integral equations which is equivalent to the concerned first order system such as the Maxwell equations or the linearized Euler equations. Using quadratures, these integral equations lead to the approximate evolution operator that builds up the evolution Galerkin scheme.

Considering the Maxwell equations in free space, it is straightforward to see that the divergence of the electric field as well as of the magnetic field is zero. Numerically, in order to have an efficient Maxwell solver, this property must be preserved. Further, the dispersion relation associated with the Maxwell equations has a key role with regard to the accuracy of the numerical scheme used.

The content of this paper is as follows: in the next section we briefly derive the exact integral equations and construct evolution Galerkin schemes. In Section 3 we write down the approximate evolution operators for the Maxwell equations. Moreover, we show that these operators preserve the divergence-free property. Further, we estimate the dispersion relation for the Maxwell EG solvers that we used. In Section 4 we derive the approximate evolution operator for the linearized Euler equations. These results presented here are the basic ingredient in our extension of the method to the case of the nonlinear Euler equations, see [6]. Finally, in Section 5 we present some numerical tests for the Maxwell equations as well as the linearized Euler equations.

2. Exact integral equations and approximate evolution operators

In this section we derive exact integral equations for a general hyperbolic system in d dimensions. Typical physical examples of hyperbolic conservation laws are, e.g., the Maxwell equations and the Euler equations of gas dynamics. Using the theory of bicharacteristics one can derive the equivalent integral equations for these systems which give a basis for the EG schemes.

Let the general form of a linear hyperbolic system be given as

$$\mathbf{U}_t + \sum_{j=1}^{d} \mathbf{A}_j \mathbf{U}_{x_j} = 0, \quad \mathbf{x} = (x_1, \dots, x_d)^T \in \mathbb{R}^d \tag{2.1}$$

where the coefficient matrices $\mathbf{A}_j$, $j = 1, \dots, d$ are elements of $\mathbb{R}^{p\times p}$ and the dependent variables are $\mathbf{U} = (u_1, \dots, u_p)^T \in \mathbb{R}^p$. Let $\mathbf{A}(\mathbf{n}) = \sum_{j=1}^{d} n_j \mathbf{A}_j$ be the *pencil matrix* with $\mathbf{n} = (n_1, \dots, n_d)^T$ being a directional vector in $\mathbb{R}^d$. Then using the eigenvectors of $\mathbf{A}(\mathbf{n})$ the system (2.1) can be written in a characteristic form via the substitution $\mathbf{W} = \mathbf{R}^{-1}\mathbf{U}$, where the columns of the matrix $\mathbf{R}$ are the linearly independent right eigenvectors of $\mathbf{A}(\mathbf{n})$. Since the coefficients of the original system are constants the bicharacteristics of the resulting characteristic system are straight lines PQ_i and PP', see Fig. 1. Diagonalizing this system and integrating along the bicharacteristics leads to the system of integral equations

$$\mathbf{U}(P) = \frac{1}{|O|}\int_O \mathbf{R}(\mathbf{n})\mathbf{W}(Q(\mathbf{n}),\mathbf{n})\,\mathrm{d}O + \frac{1}{|O|}\int_O\int_0^{\Delta t} \mathbf{R}(\mathbf{n})\mathbf{S}(t+\tau,\mathbf{n})\,\mathrm{d}\tau\,\mathrm{d}O$$

where O is the unit sphere in $\mathbb{R}^d$, $|O|$ its surface measure and S is a nontrivial term which we call the source term; for more details see [8].

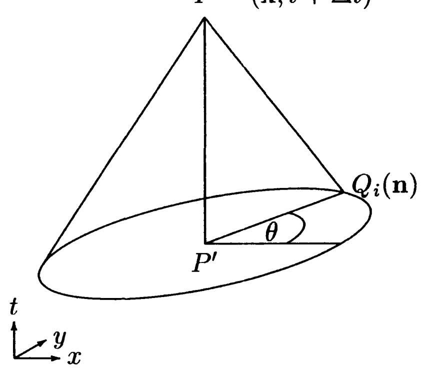

Figure 1. Bicharacteristics along the Mach cone through P and $Q_i(\mathbf{A}(\mathbf{n}))$.

Evolution Galerkin schemes

For simplicity let us consider $d = 2$. Consider $h > 0$ to be the mesh size parameter. We construct a mesh for $\mathbb{R}^2$, which consists of the square mesh cells

$$\begin{aligned}\Omega_{kl} &= \left[\left(k-\frac{1}{2}\right)h, \left(k+\frac{1}{2}\right)h\right] \times \left[\left(l-\frac{1}{2}\right)h, \left(l+\frac{1}{2}\right)h\right] \\ &= \left[x_k - \frac{h}{2}, x_k + \frac{h}{2}\right] \times \left[y_l - \frac{h}{2}, y_l + \frac{h}{2}\right],\end{aligned}$$

where $k, l \in \mathbb{Z}$. Let us denote by $H^\kappa(\mathbb{R}^2)$ the Sobolev space of distributions with derivatives up to order κ in the L^2 space, where $\kappa \in \mathbb{N}$. Consider the general hyperbolic system given by the equation (2.1). Let us denote by $E(s)\colon (H^\kappa(\mathbb{R}^2))^p \to (H^\kappa(\mathbb{R}^2))^p$ the exact evolution operator for the system (2.1), i.e.

$$\mathbf{U}(\cdot, t+s) = E(s)\mathbf{U}(\cdot, t). \tag{2.2}$$

We suppose that S_h^m is a finite element space consisting of piecewise polynomials of order $m \geqslant 0$ with respect to the square mesh. Assume a constant time step, i.e. $t_n = n\Delta t$. Let $\mathbf{U}^n$ be an approximation in the space S_h^m to the exact solution $\mathbf{U}(\cdot, t_n)$ at time $t_n \geqslant 0$. We consider $E_\tau\colon L^1_{\mathrm{loc}}(\mathbb{R}^2) \to (H^\kappa(\mathbb{R}^2))^p$ to be a suitable approximate evolution operator for $E(\tau)$. In practice we will use restrictions of E_τ to the subspace S_h^m for $m \geqslant 0$. Then we can define the general class of evolution Galerkin methods.

Definition 2.1. Starting from some initial data $\mathbf{U}^0 \in S_h^m$ at time $t = 0$, an *evolution Galerkin method (EG-method)* is recursively defined by means of

$$\mathbf{U}^{n+1} = P_h E_\tau \mathbf{U}^n, \tag{2.3}$$

where P_h is the L^2-projection given by the integral averages in the following way:

$$P_h \mathbf{U}^n|_{\Omega_{kl}} = \frac{1}{|\Omega_{kl}|} \int_{\Omega_{kl}} \mathbf{U}(x, y, t_n)\, \mathrm{d}x\, \mathrm{d}y.$$

We denote by $R_h\colon S_h^m \to S_h^r$ a recovery operator, $r \geqslant m \geqslant 0$ and consider our approximate evolution operator E_τ on S_h^r. We will limit our further considerations to the case where $m = 0$ and $r = 2$. Taking piecewise constants the resulting schemes will only be of the first order, even when E_τ is approximated to a higher order. Higher order accuracy can be obtained either by taking $m > 0$, or by inserting a recovery stage R_h before the evolution step in equation (2.3) to obtain

$$\mathbf{U}^{n+1} = P_h E_\tau R_h \mathbf{U}^n. \tag{2.4}$$

This approach involves the computation of multiple integrals and becomes quite complex for higher order recoveries. To avoid this we will consider higher order evolution Galerkin schemes based on the finite volume formulation instead.

Definition 2.2. Starting from some initial data $\mathbf{U}^0 \in S_h^m$, the finite volume evolution Galerkin method (FVEG) is recursively defined by means of

$$\mathbf{U}^{n+1} = \mathbf{U}^n - \frac{1}{h} \int_0^{\Delta t} \sum_{j=1}^{2} \delta_{x_j} \mathbf{f}_j(\tilde{\mathbf{U}}^{n+\tau/\Delta t})\, \mathrm{d}\tau, \tag{2.5}$$

where $\delta_{x_j} \mathbf{f}_j(\tilde{\mathbf{U}}^{n+\tau/\Delta t})$ represents an approximation to the edge flux difference and δ_x is defined by $\delta_x = v(x + \frac{1}{2}h) - v(x - \frac{1}{2}h)$. The cell boundary value $\tilde{\mathbf{U}}^{n+\tau/\Delta t}$ is evolved using the approximate evolution operator E_τ to $t_n + \tau$ and averaged along the cell boundary, i.e.

$$\tilde{\mathbf{U}}^{n+\tau/\Delta t} = \sum_{k,l \in \mathbb{Z}} \left(\frac{1}{|\partial\Omega_{kl}|} \int_{\partial\Omega_{kl}} E_\tau R_h \mathbf{U}^n\, \mathrm{d}S \right) \chi_{kl}, \tag{2.6}$$

where χ_{kl} is the characteristic function of $\partial\Omega_{kl}$.

In this formulation a first order approximation E_τ to the exact operator $E(\tau)$ yields an overall higher order update from $\mathbf{U}^n$ to $\mathbf{U}^{n+1}$. To obtain this approximation in the discrete scheme it is only necessary to carry out a recovery stage at each level to generate a piecewise polynomial approximation $\tilde{\mathbf{U}}^n = R_h \mathbf{U}^n \in S_h^r$ from the piecewise constant $\mathbf{U}^n \in S_h^0$, to feed into the calculation of the fluxes. To construct the second order FVEG schemes, for example, we take the first order accurate approximate evolution operator and define a bilinear reconstruction R_h. Among many possible recovery schemes which can be used, we will choose a discontinuous bilinear recovery using four point averages at each vertex. It is given as

$$\begin{aligned} R_h \mathbf{U}|_{\Omega_{kl}} &= \mathbf{U}_{kl} + \frac{x - x_k}{4h}(\Delta_{0x}\mathbf{U}_{kl+1} + 2\Delta_{0x}\mathbf{U}_{kl} + \Delta_{0x}\mathbf{U}_{kl-1}) \\ &+ \frac{y - y_l}{4h}(\Delta_{0y}\mathbf{U}_{k+1l} + 2\Delta_{0y}\mathbf{U}_{kl} + \Delta_{0y}\mathbf{U}_{k-1l}) \\ &+ \frac{(x - x_k)(y - y_l)}{h^2}\Delta_{0y}\Delta_{0x}\mathbf{U}_{kl}, \end{aligned}$$

where $\Delta_{0z} v(z) = \frac{1}{2}\big(v(z + h) - v(z - h)\big)$. Note that in the updating step (2.5) some numerical quadratures are used instead of the exact time integration. Similarly, to evaluate the intermediate value $\tilde{\mathbf{U}}^{n+\tau/\Delta t}$ in (2.6) the two dimensional integrals along the cell-interface and around the Mach cone are evaluated either exactly or by means of suitable numerical quadratures.

To close this section note that in this paper we set T to be the absolute end time of computation, i.e. $T = n\Delta t$. Further, the Courant, Friedrichs and Lewy stability number is denoted by ν and we take it to be $\nu = c\Delta t/h$ for the Maxwell equations. For the linearized Euler equation we set $\nu = \min(|u'| + c', |v'| + c')\Delta t/h$, where u', v' are the mean flows in the x and y directions respectively and c' is the local sound speed.

3. Maxwell equations

For the fundamentals of the electromagnetic theory and the Maxwell equations see Jackson [3], Balanis [1], Cheng [2]. Throughout this section we will consider the transverse magnetic (TM) modes of the electromagnetic fields only. So let us take $\mathbf{E} = E^z\hat{\mathbf{z}}$, $\mathbf{H} = H^x\hat{\mathbf{x}} + H^y\hat{\mathbf{y}}$, where $\hat{\mathbf{x}}$, $\hat{\mathbf{y}}$, $\hat{\mathbf{z}}$ are unit vectors in the direction of x, y, and z, respectively. In free space the Maxwell equations

$$\begin{aligned} \frac{\partial \mathbf{B}}{\partial t} + \nabla \times \mathbf{E} &= 0, \\ -\frac{\partial \mathbf{D}}{\partial t} + \nabla \times \mathbf{H} &= 0 \end{aligned}$$

are reduced to

$$\frac{\partial E^z}{\partial t} = \frac{1}{\varepsilon}\Big(\frac{\partial H^y}{\partial x} - \frac{\partial H^x}{\partial y}\Big), \tag{3.1}$$

$$\frac{\partial H^y}{\partial t} = \frac{1}{\mu}\frac{\partial E^z}{\partial x}, \tag{3.2}$$

$$\frac{\partial H^x}{\partial t} = -\frac{1}{\mu}\frac{\partial E^z}{\partial y}. \tag{3.3}$$

Here **E** denotes the electric field, **B** is the magnetic field, **D**, **H** denote the electric field density and magnetic field intensity, respectively. Further, we have $\mathbf{D} = \varepsilon\mathbf{E}$, $\mathbf{B} = \mu\mathbf{H}$, where ε is the permittivity and μ the permeability of the free space. Using the transformations $\varphi = E^z/\sqrt{\mu}$, $u = -H^y/\sqrt{\varepsilon}$, $v = H^x/\sqrt{\varepsilon}$ and taking $c = 1/\sqrt{\varepsilon\mu}$ equations (3.1)–(3.3) are reduced to the two dimensional wave equation system

$$\begin{aligned} \varphi_t + c(u_x + v_y) &= 0,\\ u_t + c\varphi_x &= 0,\\ v_t + c\varphi_y &= 0. \end{aligned} \tag{3.4}$$

Lukáčová et.al. [5] analyzed the evolution Galerkin schemes for the system (3.4). Namely, they derived the schemes EG1, EG2 and EG3. Moreover, in [11] the author derived the EG4 scheme. Note that the system (3.4) has the following property of irrotationality:

$$\frac{\mathrm{d}}{\mathrm{d}t}(u_y - v_x) = u_{ty} - v_{tx} = -c(\varphi_{xy} - \varphi_{yx}) = 0,$$

i.e. a solution with $u_y - v_x = 0$ for time $t = 0$ satisfies this equation of irrotationality for later times also. From the above we see that

$$0 = u_y - v_x = \frac{-1}{\sqrt{\varepsilon}}[(H^y)_y + (H^x)_x] = \frac{-1}{\sqrt{\varepsilon}}\nabla\cdot\mathbf{H}.$$

So the vorticity $u_y - v_x$ for the wave equation system corresponds to the divergence of the magnetic field. Using the above transformations we arrived at the following approximate evolution operators for the Maxwell equations.

Based on the EG4 scheme

$$(3.5)\quad E^z(P) = \frac{1}{2}\pi \int_0^{2\pi} [E^z(Q) + Z(2\cos\theta H^y(Q) - 2\sin\theta H^x(Q))]\,\mathrm{d}\theta + \mathcal{O}(\Delta t^2),$$

$$(3.6)\quad H^y(P) = \frac{1}{2\pi} \int_0^{2\pi} \Big[\frac{2\cos\theta E^z(Q)}{Z} + 2\cos^2\theta H^y(Q) - 2\sin\theta\cos\theta H^x(Q)\Big]\,\mathrm{d}\theta + \mathcal{O}(\Delta t^2),$$

$$(3.7)\quad H^x(P) = \frac{1}{2\pi} \int_0^{2\pi} \Big[\frac{-2\sin\theta E^z(Q)}{Z} - 2\sin\theta\cos\theta H^y(Q) + 2\sin^2\theta H^x(Q)\Big]\,\mathrm{d}\theta + \mathcal{O}(\Delta t^2).$$

Based on the EG3 scheme

$$(3.8)\qquad E^z(P) = \frac{1}{2\pi} \int_0^{2\pi} [E^z(Q) + Z(2\cos\theta H^y(Q) - 2\sin\theta H^x(Q))]\,\mathrm{d}\theta + \mathcal{O}(\Delta t^2),$$

$$(3.9)\qquad H^y(P) = \frac{1}{2}H^y(P') + \frac{1}{2\pi} \int_0^{2\pi} \Big[\frac{2\cos\theta E^z(Q)}{Z} + (3\cos^2\theta - 1)H^y(Q) - 3\sin\theta\cos\theta H^x(Q)\Big]\,\mathrm{d}\theta + \mathcal{O}(\Delta t^2),$$

$$(3.10)\qquad H^x(P) = \frac{1}{2}H^x(P') + \frac{1}{2\pi} \int_0^{2\pi} \Big[\frac{-2\sin\theta E^z(Q)}{Z} - 3\sin\theta\cos\theta H^y(Q) + (3\sin^2\theta - 1)H^x(Q)\Big]\,\mathrm{d}\theta + \mathcal{O}(\Delta t^2),$$

where $Z = \sqrt{\mu/\varepsilon}$ is the so-called impedance of free space. Taking the projection onto piecewise constant functions we obtain the evolution Galerkin schemes for the Maxwell equations. Numerical schemes based on equations (3.5)—(3.7) and (3.8)–(3.10) are called the EG4 and the EG3 methods, respectively. Note that these schemes are first order schemes. In order to have second order methods for the Maxwell equations we use the finite volume formulation as given in Definition 2.2. Assuming the periodicity of the fields in space we get the following two lemmas.

Lemma 3.1. *The approximate evolution operators for the Maxwell equations* EG3 *and* EG4 *are divergence-free.*

Proof. We prove only the case of the EG4 scheme, the EG3 scheme can be treated analogously. To this end, $\nabla \cdot \mathbf{E} = 0$ follows immediately from the assumption that $\mathbf{E} = E^z(x, y, t)\hat{\mathbf{z}}$. Now taking the derivatives with respect to y and x of the equations (3.6) and (3.7), respectively we get

(3.11)

$$\frac{\partial H^y}{\partial y}(P) = \frac{1}{2\pi}\int_0^{2\pi}\Big(\frac{2\cos\theta}{Z}\frac{\partial E^z}{\partial y}(Q) + 2\cos^2\theta\frac{\partial H^y}{\partial y}(Q) - 2\sin\theta\cos\theta\frac{\partial H^x}{\partial y}(Q)\Big)\,\mathrm{d}\theta,$$

(3.12)

$$\frac{\partial H^x}{\partial x}(P) = \frac{1}{2\pi}\int_0^{2\pi}\Big(\frac{-2\sin\theta}{Z}\frac{\partial E^z}{\partial x}(Q) - 2\sin\theta\cos\theta\frac{\partial H^y}{\partial x}(Q) + 2\sin^2\theta\frac{\partial H^x}{\partial x}(Q)\Big)\,\mathrm{d}\theta.$$

Adding equation (3.11) to the equation (3.12) we obtain

$$\begin{aligned}(3.13)\quad \frac{\partial H^x}{\partial x}(P) + \frac{\partial H^y}{\partial y}(P) = \frac{1}{2\pi}\int_0^{2\pi}&\Big[\frac{2}{Z}\Big(\cos\theta\frac{\partial E^z}{\partial y}(Q) - \sin\theta\frac{\partial E^z}{\partial x}(Q)\Big)\\ &+ 2\Big(\cos^2\theta\frac{\partial H^y}{\partial y}(Q) - \sin\theta\cos\theta\frac{\partial H^y}{\partial x}(Q)\Big)\\ &+ 2\Big(\sin^2\theta\frac{\partial H^x}{\partial x}(Q) - \sin\theta\cos\theta\frac{\partial H^x}{\partial y}(Q)\Big)\Big]\,\mathrm{d}\theta.\end{aligned}$$

Now the integral of the first term of equation (3.13) is zero because

$$\begin{aligned}&\int_0^{2\pi}\frac{2}{Z}\Big(\cos\theta\frac{\partial E^z}{\partial y}(Q) - \sin\theta\frac{\partial E^z}{\partial x}(Q)\Big)\,\mathrm{d}\theta\\ &\qquad = \int_0^{2\pi}\frac{2}{Z}(-\sin\theta,\cos\theta)^T\cdot\nabla E^z\,\mathrm{d}\theta = \int_0^{2\pi}\frac{2}{Z}dE^z\end{aligned}$$

and $\mathbf{E}$ is a periodic field. We use the periodicity of the magnetic field $\mathbf{H}$ and the fact that the initial data are divergence-free. Then integration by parts gives

$$\begin{aligned}(3.14)\quad &\int_0^{2\pi}\Big(\cos^2\theta\frac{\partial H^y}{\partial y}(Q) - \sin\theta\cos\theta\frac{\partial H^y}{\partial x}(Q)\Big)\,\mathrm{d}\theta\\ &\qquad = \int_0^{2\pi}\cos\theta\Big(\frac{\partial H^y}{\partial y}(Q) - \sin\theta\frac{\partial H^y}{\partial x}(Q)\Big)\,\mathrm{d}\theta\\ &\qquad = \int_0^{2\pi}\cos\theta(-\sin\theta,\cos\theta)^T\cdot\nabla H^y(Q)\,\mathrm{d}\theta\\ &\qquad = \int_0^{2\pi}\cos\theta\frac{dH^y}{d\theta}(Q)\,\mathrm{d}\theta = \int_0^{2\pi}\sin\theta H^y(Q)\,\mathrm{d}\theta.\end{aligned}$$

Analogously we have

$$(3.15)\quad \int_0^{2\pi}\Big(\sin^2\theta\frac{\partial H^x}{\partial x}(Q) - \sin\theta\cos\theta\frac{\partial H^x}{\partial y}(Q)\Big)\,\mathrm{d}\theta = \int_0^{2\pi}\cos\theta H^x(Q)\,\mathrm{d}\theta.$$

Summing equations (3.14) and (3.15) we get

$$\int_0^{2\pi}\Big(\sin^2\theta\frac{\partial H^x}{\partial x}(Q)-\sin\theta\cos\theta\frac{\partial H^y}{\partial x}(Q)+\cos^2\theta\frac{\partial H^y}{\partial y}(Q)-\sin\theta\cos\theta\frac{\partial H^x}{\partial y}(Q)\Big)\,\mathrm{d}\theta$$
$$=\int_0^{2\pi}(\cos\theta H^x(Q)+\sin\theta H^y(Q))d\theta$$
$$=\int_0^{2\pi}\mathbf{H}(Q)\cdot\mathbf{n}\,\mathrm{d}\theta=\oint\nabla\cdot\mathbf{H}(Q)\,\mathrm{d}S=0.$$

Therefore $\nabla\cdot\mathbf{H}=0$. This concludes the proof of the lemma. □

Remark 3.1. Similar results hold also for other EG operators, i.e. EG1, EG2, the operator of Ostkamp, cf. [5] for the precise formulation.

Our next aim is to approximate the dispersion relation. To this end note that a frequently used technique of characterizing the error of numerical schemes of the Maxwell equations is the Fourier analysis. Neglecting the boundary conditions, we assume that the three unknown components can be expressed in the following form:

$$\psi^n_{IJ}=\psi_0\exp\big(\mathrm{i}(\tilde{\xi}Ih+\tilde{\eta}Jh-\omega n\Delta t)\big), \tag{3.16}$$

where $\mathrm{i}=\sqrt{-1}$, h is the space increment and $\tilde{\xi}$ and $\tilde{\eta}$ are the x and y components of the numerical wave vector, respectively. In the case of the exact solution this gives

$$\psi(x,y,t)=\psi_0\exp\big(\mathrm{i}(\xi x+\eta y-\omega t)\big). \tag{3.17}$$

The numerical wave vector $\tilde{\mathbf{k}}=(\tilde{\xi},\tilde{\eta})^T$ will in general differ from the physical wave vector $\mathbf{k}=(\xi,\eta)^T$ satisfying $|\mathbf{k}|=\sqrt{\xi^2+\eta^2}=\omega/c$. This is called the dispersion relation. Here ω is the angular frequency and c is the speed of light. The difference between $\mathbf{k}$ and $\tilde{\mathbf{k}}$ gives rise to numerical phase and group velocities that depart from the analytical values. This causes numerical errors that accumulate in time. Hence the dispersion analysis is important to assess the accuracy of a numerical solution. In the next lemma we study the approximation of the dispersion relation for the EG4 method in the case of Maxwell equations.

Lemma 3.2. *For both the* EG4 *method* (3.5)–(3.7) *and the* EG3 *method* (3.8)–(3.10) *the following dispersion relation holds:*

$$\Big(\frac{\omega}{c}\Big)^2=(\tilde{\xi}^2+\tilde{\eta}^2)+\mathcal{O}(h). \tag{3.18}$$

Proof. We present the proof of (3.18) for the EG4 scheme, the proof for the EG3 scheme is analogous. First we write out the finite difference formulation of the EG4 scheme:

$$(3.19)\quad E^{z^{n+1}} = (1 + a_{11}(s_x^2 + s_y^2) + b_{11}s_x^2 s_y^2)E^{z^n} + Z(\nu(1 + a_{12}s_y^2)\Delta_{0x}H^{y^n} - \nu(1 + a_{13}s_x^2)\Delta_{0y}H^{x^n}),$$

$$(3.20)\quad H^{y^{n+1}} = (1 + (a_{22}s_x^2 + a'_{22}s_y^2) + b_{22}s_x^2 s_y^2)H^{y^n} + \frac{\nu}{Z}(1 + a_{21}s_y^2)\Delta_{0x}E^{z^n} - \nu^2 a_{23}\Delta_{0x}\Delta_{0y}H^{x^n},$$

$$(3.21)\quad H^{x^{n+1}} = (1 + (a_{33}s_x^2 + a'_{33}s_y^2) + b_{33}s_x^2 s_y^2)H^{x^n} - \frac{\nu}{Z}(1 + a_{31}s_x^2)\Delta_{0y}E^{z^n} - \nu^2 a_{32}\Delta_{0x}\Delta_{0y}H^{y^n},$$

where $\nu = c\Delta t/h$, $\Delta_{0z} = \frac{1}{2}(f(z+h) - f(z-h))$, $s_z^2 = f(z+h) - 2f(z) + f(z-h)$ and

$$a_{11} = \frac{\nu}{\pi},\quad b_{11} = \frac{\nu^2}{4\pi},\quad a_{12} = \frac{2\nu}{3\pi},\quad a_{13} = \frac{2\nu}{3\pi},$$
$$a_{21} = \frac{2\nu}{3\pi},\quad a_{22} = \frac{4\nu}{3\pi},\quad a'_{22} = \frac{2\nu}{3\pi},\quad b_{22} = \frac{\nu^2}{4\pi},\quad a_{23} = \frac{1}{4},$$
$$a_{31} = \frac{2\nu}{3\pi},\quad a_{32} = \frac{1}{4},\quad a_{33} = \frac{2\nu}{3\pi},\quad a'_{33} = \frac{4\nu}{3\pi},\quad b_{33} = \frac{\nu^2}{4\pi}.$$

Substituting from equation (3.16) into equations (3.19)–(3.21) we get

$$(3.22)\quad \begin{aligned} -\mathrm{i}\omega\Delta t = {} & 2a_{11}(\cos(h\tilde{\xi}) - 1) + 2a_{11}(\cos(h\tilde{\eta}) - 1) \\ & + 4b_{11}(\cos(h\tilde{\xi}) - 1)(\cos(h\tilde{\eta}) - 1) \\ & + \mathrm{i}Z\nu\frac{H_0^y}{E_0^z}\sin(h\tilde{\xi})[1 + 2a_{12}(\cos(h\tilde{\eta}) - 1)] \\ & - \mathrm{i}Z\nu\frac{H_0^x}{E_0^z}\sin(h\tilde{\eta})[1 + 2a_{13}(\cos(h\tilde{\xi}) - 1)], \end{aligned}$$

$$(3.23)\quad \begin{aligned} -\mathrm{i}\omega\Delta t = {} & 2a_{22}(\cos(h\tilde{\xi}) - 1) + 2a'_{22}(\cos(h\tilde{\eta}) - 1) \\ & + 4b_{22}(\cos(h\tilde{\xi}) - 1)(\cos(h\tilde{\eta}) - 1) \\ & + \mathrm{i}\frac{\nu}{Z}\frac{E_0^z}{H_0^y}\sin(h\tilde{\xi})[1 + 2a_{21}(\cos(h\tilde{\eta}) - 1)] \\ & + \nu^2 a_{23}\frac{H_0^x}{H_0^y}\sin(h\tilde{\eta})\sin(h\tilde{\xi}), \end{aligned}$$

$$(3.24)\quad \begin{aligned} -\mathrm{i}\omega\Delta t = {} & 2a_{33}(\cos(h\tilde{\xi}) - 1) + 2a'_{33}(\cos(h\tilde{\eta}) - 1) \\ & + 4b_{33}(\cos(h\tilde{\xi}) - 1)(\cos(h\tilde{\eta}) - 1) \end{aligned}$$

$$-\mathrm{i}\,\frac{\nu}{Z}\frac{E_0^z}{H_0^x}\sin(h\tilde{\eta})[1+2a_{31}(\cos(h\tilde{\xi})-1)]$$
$$+\,\nu^2 a_{32}\frac{H_0^y}{H_0^x}\sin(h\tilde{\eta})\sin(h\tilde{\xi}).$$

Now equations (3.23) and (3.24) imply, respectively, that

$$\frac{H_0^y}{E_0^z}=\frac{\frac{\nu}{Z}\sin(h\tilde{\xi})[1+2a_{21}(\cos(h\tilde{\eta})-1)]}{-\omega\Delta t+\mathrm{i}[\alpha+\nu^2 a_{23}\frac{H_0^x}{H_0^y}\sin(h\tilde{\xi})\sin(h\tilde{\eta})]},\tag{3.25}$$

$$\frac{H_0^x}{E_0^z}=\frac{\frac{\nu}{Z}\sin(h\tilde{\eta})[1+2a_{31}(\cos(h\tilde{\xi})-1)]}{\omega\Delta t-\mathrm{i}[\beta+\nu^2 a_{32}\frac{H_0^y}{H_0^x}\sin(h\tilde{\xi})\sin(h\tilde{\eta})]},\tag{3.26}$$

where

$$\alpha:=2a_{22}(\cos(h\tilde{\xi})-1)+2a_{22}'(\cos(h\tilde{\eta})-1)+4b_{22}(\cos(h\tilde{\xi})-1)(\cos(h\tilde{\eta})-1),$$
$$\beta:=2a_{33}(\cos(h\tilde{\xi})-1)+2a_{33}'(\cos(h\tilde{\eta})-1)+4b_{33}(\cos(h\tilde{\xi})-1)(\cos(h\tilde{\eta})-1).$$

Substituting equations (3.25) and (3.26) into equation (3.22) leads to

$$\omega\Delta t=\mathrm{i}\gamma-\frac{\nu^2\sin^2(h\tilde{\xi})(1+2a_{12}(\cos(h\tilde{\eta})-1))^2}{-\omega\Delta t+\mathrm{i}(\alpha+\nu^2 a_{23}\frac{H_0^x}{H_0^y}\sin(h\tilde{\xi})\sin(h\tilde{\eta}))}$$
$$-\frac{\nu^2\sin^2(h\tilde{\eta})(1+2a_{13}(\cos(h\tilde{\xi})-1))^2}{-\omega\Delta t+\mathrm{i}(\beta+\nu^2 a_{32}\frac{H_0^y}{H_0^x}}\sin(h\tilde{\xi})\sin(h\tilde{\eta})),\tag{3.27}$$

where

$$\gamma:=2a_{11}(\cos(h\tilde{\xi})-1)+2a_{11}(\cos(h\tilde{\eta})-1)+4b_{11}(\cos(h\tilde{\xi})-1)(\cos(h\tilde{\eta})-1).$$

Equation (3.27) can be written in the form

$$\begin{aligned}(\omega\Delta t-\mathrm{i}\gamma)\Big(-\omega\Delta t+\mathrm{i}\Big[\alpha+\nu^2 a_{23}\frac{H_0^x}{H_0^y}\sin(h\tilde{\xi})\sin(h\tilde{\eta})\Big]\Big)&\\ \times\Big(-\omega\Delta t+\mathrm{i}\Big[\beta+\nu^2 a_{32}\frac{H_0^y}{H_0^x}\sin(h\tilde{\xi})\sin(h\tilde{\eta})\Big]\Big)&\\ =-\nu^2\sin^2(h\tilde{\xi})[1+2a_{12}(\cos(h\tilde{\eta})-1)]^2&\\ \times\Big(-\omega\Delta t+\mathrm{i}\Big[\beta+\nu^2 a_{32}\frac{H_0^y}{H_0^x}\sin(h\tilde{\xi})\sin(h\tilde{\eta})\Big]\Big)&\\ -\nu^2\sin^2(h\tilde{\eta})[1+2a_{13}(\cos(h\tilde{\xi})-1)]^2&\\ \times\Big(-\omega\Delta t+\mathrm{i}\Big[\alpha+\nu^2 a_{23}\frac{H_0^x}{H_0^y}\sin(h\tilde{\xi})\sin(h\tilde{\eta})\Big]\Big).&\end{aligned}\tag{3.28}$$

Using the Taylor expansion we can show that γ, α and β are of order $\nu^2\mathcal{O}(h^2)$ and $\sin(hx)=hx+\mathcal{O}(h^3)$. The left- and the right-hand sides of equation (3.28) can be written as

$$
\begin{aligned}
\text{LHS} = &\Big(-\omega^2\Delta t^2 + \mathrm{i}\omega\gamma\Delta t + \mathrm{i}\omega\Delta t\Big[\alpha + \nu^2 a_{23}\frac{H_0^x}{H_0^y}\sin(h\tilde{\xi})\sin(h\tilde{\eta})\Big]\Big) \\
&+ \gamma\Big[\alpha + \nu^2 a_{23}\frac{H_0^x}{H_0^y}\sin(h\tilde{\xi})\sin(h\tilde{\eta})\Big] \\
&\times \Big(-\omega\Delta t + \mathrm{i}\Big[\beta + \nu^2 a_{32}\frac{H_0^y}{H_0^x}\sin(h\tilde{\xi})\sin(h\tilde{\eta})\Big]\Big) \\
= &\ \omega^3\Delta t^3 - \mathrm{i}\omega^2\Delta t^2\Big[\beta + \nu^2 a_{32}\frac{H_0^y}{H_0^x}\sin(h\tilde{\xi})\sin(h\tilde{\eta})\Big] - \mathrm{i}\omega^2\Delta t^2\,\gamma \\
&- \gamma\omega\Delta t\Big[\beta + \nu^2 a_{32}\frac{H_0^y}{H_0^x}\sin(h\tilde{\xi})\sin(h\tilde{\eta})\Big] \\
&- \mathrm{i}\omega^2\Delta t^2\Big[\alpha + \nu^2 a_{23}\frac{H_0^x}{H_0^y}\sin(h\tilde{\xi})\sin(h\tilde{\eta})\Big] \\
&- \omega\Delta t\Big[\alpha + \nu^2 a_{23}\frac{H_0^x}{H_0^y}\sin(h\tilde{\xi})\sin(h\tilde{\eta})\Big]\Big[\beta + \nu^2 a_{32}\frac{H_0^y}{H_0^x}\sin(h\tilde{\xi})\sin(h\tilde{\eta})\Big] \\
&- \omega\Delta t\gamma[\alpha + \nu^2 a_{23}\frac{H_0^x}{H_0^y}\sin(h\tilde{\xi})\sin(h\tilde{\eta})] \\
&+ \mathrm{i}\gamma\Big[\alpha + \nu^2 a_{23}\frac{H_0^x}{H_0^y}\sin(h\tilde{\xi})\sin(h\tilde{\eta})\Big]\Big[\beta + \nu^2 a_{32}\frac{H_0^y}{H_0^x}\sin(h\tilde{\xi})\sin(h\tilde{\eta})\Big] \\
= &\ \omega^3\Delta t^3 + \nu^2\omega\Delta t\mathcal{O}(h^3), \\
\text{RHS} = &\ \nu^2\omega\Delta t\sin^2(h\tilde{\xi}) - \nu^2\sin^2(h\tilde{\xi})\mathrm{i}\Big[\beta + \nu^2 a_{32}\frac{H_0^y}{H_0^x}\sin(h\tilde{\xi})\sin(h\tilde{\eta})\Big] \\
&+ \nu^2\omega\Delta t\sin^2(h\tilde{\xi})4a_{12}(\cos(h\tilde{\eta}) - 1) \\
&-\mathrm{i}\nu^2\sin^2(h\tilde{\xi})4a_{12}(\cos(h\tilde{\eta}) - 1)\Big[\beta + \nu^2 a_{32}\frac{H_0^y}{H_0^x}\sin(h\tilde{\xi})\sin(h\tilde{\eta})\Big] \\
&+ \nu^2\omega\Delta t\sin^2(h\tilde{\xi})4a_{12}^2(\cos(h\tilde{\eta}) - 1)^2 \\
&-\mathrm{i}\nu^2\omega\Delta t\sin^2(h\tilde{\xi})4a_{12}^2(\cos(h\tilde{\eta}) - 1)^2\Big[\beta + \nu^2 a_{32}\frac{H_0^y}{H_0^x}\sin(h\tilde{\xi})\sin(h\tilde{\eta})\Big] \\
&+ \nu^2\omega\Delta t\sin^2(h\tilde{\eta}) - \nu^2\sin^2(h\tilde{\eta})\mathrm{i}\Big[\alpha + \nu^2 a_{23}\frac{H_0^x}{H_0^y}\sin(h\tilde{\xi})\sin(h\tilde{\eta})\Big] \\
&+ \nu^2\omega\Delta t\sin^2(h\tilde{\eta})4a_{13}(\cos(h\tilde{\xi}) - 1) \\
&-\mathrm{i}\nu^2\sin^2(h\tilde{\eta})4a_{13}(\cos(h\tilde{\xi}) - 1)\Big[\alpha + \nu^2 a_{23}\frac{H_0^x}{H_0^y}\sin(h\tilde{\xi})\sin(h\tilde{\eta})\Big] \\
&+ \nu^2\omega\Delta t\sin^2(h\tilde{\eta})4a_{13}^2(\cos(h\tilde{\xi}) - 1)^2 \\
&-\mathrm{i}\nu^2\omega\Delta t\sin^2(h\tilde{\eta})4a_{13}^2(\cos(h\tilde{\xi}) - 1)^2\Big[\alpha + \nu^2 a_{23}\frac{H_0^x}{H_0^y}\sin(h\tilde{\xi})\sin(h\tilde{\eta})\Big] \\
= &\ \nu^2\omega\Delta t[\sin^2(h\tilde{\xi}) + \sin^2(h\tilde{\eta})] + \nu^2\omega\Delta t\mathcal{O}(h^3).
\end{aligned}
$$

Therefore we have

$$\omega^3 \Delta t^3 = \nu^2 \omega \Delta t [\sin^2(h\tilde{\xi}) + \sin^2(h\tilde{\eta})] + \mathcal{O}(h^3). \tag{3.29}$$

Finally, equation (3.29) leads to (3.18), which concludes the proof. □

4. Approximate evolution operators for linearized Euler equations in 2D

In this section we derive an evolution Galerkin scheme for the linearized Euler equations of gas dynamics written in primitive variables. This will be used in [6] for the fully nonlinear case. This scheme is similar to the EG4 scheme for the two-dimensional wave equation system. To define it we consider the linearized Euler equations with frozen coefficients

$$\mathbf{U}_t + \mathbf{A}_1(\mathbf{U}')\mathbf{U}_x + \mathbf{A}_2(\mathbf{U}')\mathbf{U}_y = 0, \quad \mathbf{x} = (x, y)^T \in \mathbb{R}^2, \tag{4.1}$$

where

$$\mathbf{U} := \begin{pmatrix} \varrho \\ u \\ v \\ p \end{pmatrix}, \quad \mathbf{U}' := \begin{pmatrix} \varrho' \\ u' \\ v' \\ p' \end{pmatrix}, \quad \mathbf{A}_1 := \begin{pmatrix} u' & \varrho' & 0 & 0 \\ 0 & u' & 0 & 1/\varrho' \\ 0 & 0 & u' & 0 \\ 0 & \varrho'(c')^2 & 0 & u' \end{pmatrix},$$

$$\mathbf{A}_2 := \begin{pmatrix} v' & 0 & \varrho' & 0 \\ 0 & v' & 0 & 0 \\ 0 & 0 & v' & 1/\varrho' \\ 0 & 0 & \varrho'(c')^2 & v' \end{pmatrix}.$$

Here ϱ denotes the density, u and v denote the two components of the velocity vector and p denotes the pressure. Symbols ϱ', u', v' and p' stay for the local variables at a point (x', y'), $c' = \sqrt{\gamma p'/\varrho'}$ is the local speed of the sound there and γ is the isotropic exponent ($\gamma = 1.4$ for the dry air). We use the theory presented in Section 2 to derive the integral equations that correspond to the system (4.1), see also [4], [6] for the derivation of other approximate evolution operators for the Euler equations. Thus we take the direction $\mathbf{n}(\theta) := (\cos\theta, \sin\theta)^T$ in $\mathbb{R}^2$ and define the pencil matrix to be $\mathbf{A}(\mathbf{n}) := \mathbf{A}_1 \cos\theta + \mathbf{A}_2 \sin\theta$. The eigenvectors of $\mathbf{A}(\mathbf{n})$ are

$$\begin{aligned} \lambda_1 &= u' \cos\theta + v' \sin\theta - c', \\ \lambda_2 = \lambda_3 &= u' \cos\theta + v' \sin\theta, \\ \lambda_4 &= u' \cos\theta + v' \sin\theta + c', \end{aligned}$$

and the corresponding right eigenvectors are

$$\mathbf{r}_1 = \begin{pmatrix} -\varrho'/c' \\ \cos\theta \\ \sin\theta \\ -\varrho'c' \end{pmatrix}, \quad \mathbf{r}_2 = \begin{pmatrix} 1 \\ 0 \\ 0 \\ 0 \end{pmatrix}, \quad \mathbf{r}_3 = \begin{pmatrix} 0 \\ \sin\theta \\ -\cos\theta \\ 0 \end{pmatrix}, \quad \mathbf{r}_4 = \begin{pmatrix} \varrho'/c' \\ \cos\theta \\ \sin\theta \\ \varrho'c' \end{pmatrix}.$$

Take the matrix $\mathbf{R}$ to be the matrix of the right eigenvectors. Then multiplying system (4.1) from the left by the inverse matrix

$$\mathbf{R}^{-1} = \begin{pmatrix} 0 & \cos\theta & \sin\theta & -1/(2\varrho'c') \\ 1 & 0 & 0 & -1/c'^2 \\ 0 & \sin\theta & -\cos\theta & 0 \\ 0 & \cos\theta & \sin\theta & 1/(2\varrho'c') \end{pmatrix}$$

we get the characteristic system

$$\mathbf{W}_t + \mathbf{B}_1\mathbf{W}_x + \mathbf{B}_2\mathbf{W}_y = 0, \tag{4.2}$$

where

$$\mathbf{W} = \begin{pmatrix} w_1 \\ w_2 \\ w_3 \\ w_4 \end{pmatrix} = \mathbf{R}^{-1}\mathbf{U} = \begin{pmatrix} \frac{1}{2}\left(-p/(\varrho'c') + u\cos\theta + v\sin\theta\right) \\ \varrho - p/c'^2 \\ u\cos\theta - v\sin\theta \\ \frac{1}{2}\left(p/(\varrho'c') + u\cos\theta + v\sin\theta\right) \end{pmatrix}$$

is the vector of the characteristic variables and

$$\mathbf{B}_1 = \mathbf{R}^{-1}\mathbf{A}_1\mathbf{R} = \begin{pmatrix} u' - c'\cos\theta & 0 & -\frac{1}{2}c'\sin\theta & 0 \\ 0 & u' & 0 & 0 \\ -c'\sin\theta & 0 & u' & c'\sin\theta \\ 0 & 0 & \frac{1}{2}c'\sin\theta & u' + c'\cos\theta \end{pmatrix},$$

$$\mathbf{B}_2 = \mathbf{R}^{-1}\mathbf{A}_2\mathbf{R} = \begin{pmatrix} v' - c'\sin\theta & 0 & \frac{1}{2}c'\cos\theta & 0 \\ 0 & v' & 0 & 0 \\ c'\cos\theta & 0 & v' & -c'\cos\theta \\ 0 & 0 & -\frac{1}{2}c'\cos\theta & v' + c'\sin\theta \end{pmatrix}.$$

Diagonalizing system (4.2) we end up with

$$\mathbf{W}_t + \mathbf{\Lambda}_1\mathbf{W}_x + \mathbf{\Lambda}_2\mathbf{W}_y = \mathbf{S}, \tag{4.3}$$

where

$$\mathbf{S} = \begin{pmatrix} S_1 \\ S_2 \\ S_3 \\ S_4 \end{pmatrix} = \begin{pmatrix} \frac{1}{2}c'\left(\sin\theta\,\partial w_3/\partial x - \cos\theta\,\partial w_3/\partial y\right) \\ 0 \\ c'\sin\theta\left(\partial w_1/\partial x - \partial w_4/\partial x\right) - c'\cos\theta\left(\partial w_1/\partial y - \partial w_4/\partial y\right) \\ \frac{1}{2}c'\left(-\sin\theta\,\partial w_3/\partial x + \cos\theta\,\partial w_3/\partial y\right) \end{pmatrix}$$

and

$$\mathbf{\Lambda}_1 = \begin{pmatrix} u' - c'\cos\theta & 0 & 0 & 0 \\ 0 & u' & 0 & 0 \\ 0 & 0 & u' & 0 \\ 0 & 0 & 0 & u' + c'\cos\theta \end{pmatrix},$$

$$\mathbf{\Lambda}_2 = \begin{pmatrix} v' - c'\sin\theta & 0 & 0 & 0 \\ 0 & v' & 0 & 0 \\ 0 & 0 & v' & 0 \\ 0 & 0 & 0 & v' + c'\sin\theta \end{pmatrix}.$$

Let us define the bicharacteristics $\mathbf{x}_1$, $\mathbf{x}_2$, $\mathbf{x}_3$, $\mathbf{x}_4$ corresponding to each equation of system (4.3) as

$$\begin{aligned} \frac{\mathrm{d}\mathbf{x}_1}{\mathrm{d}\tilde{t}} &:= (u' - c'\cos\theta, v' - c'\sin\theta)^T, \\ \frac{\mathrm{d}\mathbf{x}_2}{\mathrm{d}\tilde{t}} &:= (u', v')^T, \\ \frac{\mathrm{d}\mathbf{x}_3}{\mathrm{d}\tilde{t}} &:= (u', v')^T, \\ \frac{\mathrm{d}\mathbf{x}_4}{\mathrm{d}\tilde{t}} &:= (u' + c'\cos\theta, v' + c'\sin\theta)^T. \end{aligned}$$

Note that as θ varies from 0 to 2π the resulting geometry is a Mach cone shown in Fig. 2 for the supersonic case $c'^2 > u'^2 + v'^2$. Moreover, we use the initial data $\mathbf{x}_i(\mathbf{n}, t + \Delta t) = \mathbf{x}$ to solve the above ordinary differential equations backwards and

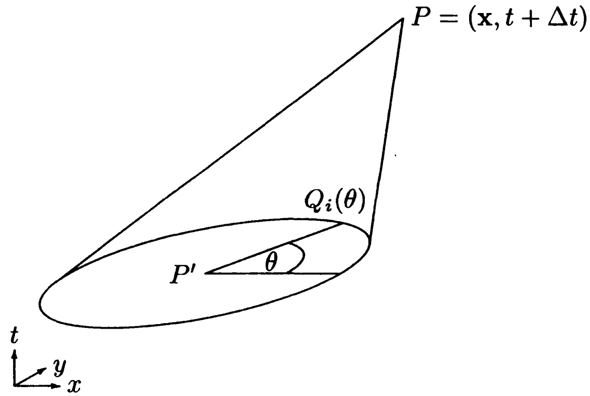

Figure 2. Bicharacteristic along the Mach cone through P and $Q_i(\theta)$, supersonic case.

get the footpoints $Q_i(\theta)$ of the bicharacteristics. The final result reads

$$Q_1 = (x - (u' - c'\cos\theta)\Delta t, y - (v' - c'\sin\theta)\Delta t, t),$$
$$Q_2 = Q_3 = P' = (x - u'\Delta t, y - v'\Delta t, t),$$
$$Q_4 = (x - (u' + c'\cos\theta)\Delta t, y - (v' + c'\sin\theta)\Delta t, t).$$

Now we integrate each equation of the characteristic system (4.3) along the corresponding bicharacteristic from the point $P = (x, y, t + \Delta t)$ down to the point Q where it hits the base of the Mach cone, see Fig. 2. Further, multiplying the resulting system by the matrix $\mathbf{R}$ from the left we obtain the following *integral equations*:

$$\text{(4.4)} \qquad \mathbf{U}_P = \frac{1}{2\pi}\int_0^{2\pi} \begin{pmatrix} -\varrho' w_1/c' + w_2 + \varrho' w_4/c' \\ w_1\cos\theta + w_3\sin\theta + w_4\cos\theta \\ w_1\cos\theta - w_3\sin\theta + w_4\cos\theta \\ -\varrho' c' w_1 + \varrho' c' w_4 \end{pmatrix} \mathrm{d}\theta$$

$$+ \frac{1}{2\pi}\int_0^{2\pi} \begin{pmatrix} -\varrho' S_1'/c' + S_2' + \varrho' S_4'/c' \\ S_1'\cos\theta + S_4'\sin\theta + S_4'\cos\theta \\ S_1'\sin\theta - S_3'\cos\theta + S_4'\sin\theta \\ -\varrho' c' S_1' + \varrho' c' S_4' \end{pmatrix} \mathrm{d}\theta,$$

where $S_i' = \int_t^{t+\Delta t} S_i(\mathbf{x}_i(\tilde{t},\theta), \tilde{t}, \theta)\,\mathrm{d}\tilde{t}$. We use the symmetry between the points Q_1 and Q_3 and the fact that the functions w_i as well as the points Q_i are 2π-periodic. Then using the notation

$$S(\mathbf{x}, t, \theta) := c'[\sin\theta^2 u_x(\mathbf{x}, t, \theta) - \sin\theta\cos\theta(u_y(\mathbf{x}, t, \theta) + v_x(\mathbf{x}, t, \theta)) + \cos\theta^2 v_y(\mathbf{x}, t, \theta)]$$

and $Q := Q_1$ we can rewrite system (4.4) in the following form:

$$\text{(4.5)} \quad \varrho(\mathbf{x}, t + \Delta t) = \varrho(P') - \frac{p(P')}{c'^2} + \frac{1}{2\pi}\int_0^{2\pi}\Big(\frac{p(Q)}{c'^2} - \frac{\varrho'}{c'}u(Q)\cos\theta - \frac{\varrho'}{c'}v(Q)\sin\theta\Big)\,\mathrm{d}\theta - \frac{\varrho'}{c'}\frac{1}{2\pi}\int_0^{2\pi}\int_0^{\Delta t} S(\mathbf{x} - (\mathbf{u}' - c'\mathbf{n}(\theta))\tau, t + \Delta t - \tau, \theta)\,\mathrm{d}\tau\,\mathrm{d}\theta,$$

$$\text{(4.6)} \quad u(\mathbf{x}, t + \Delta t) = \frac{1}{2}u(P') - \frac{1}{2\varrho'}\int_0^{\Delta t} p_x(P')\,\mathrm{d}\tau + \frac{1}{2\pi}\int_0^{2\pi}\Big(-\frac{p(Q)}{\varrho' c'}\cos\theta + u(Q)\cos^2\theta + v(Q)\sin\theta\cos\theta\Big)\,\mathrm{d}\theta + \frac{1}{2\pi}\int_0^{2\pi}\int_0^{\Delta t} \cos\theta S(\mathbf{x} - (\mathbf{u}' - c'\mathbf{n}(\theta))\tau, t + \Delta t - \tau, \theta)\,\mathrm{d}\tau\,\mathrm{d}\theta,$$

$$(4.7)\quad v(\mathbf{x},t+\Delta t) = \frac{1}{2}v(P') - \frac{1}{2\varrho'}\int_0^{\Delta t} p_y(P')\,\mathrm{d}\tau$$
$$+\frac{1}{2\pi}\int_0^{2\pi}\Big(-\frac{p(Q)}{\varrho' c'}\sin\theta + u(Q)\sin\theta\cos\theta + v(Q)\sin^2\theta\Big)\,\mathrm{d}\theta$$
$$+\frac{1}{2\pi}\int_0^{2\pi}\int_0^{\Delta t}\sin\theta S(\mathbf{x}-(\mathbf{u}'-c'\mathbf{n}(\theta))\tau, t+\Delta t-\tau,\theta)\,\mathrm{d}\tau\,\mathrm{d}\theta,$$

$$(4.8)\quad p(\mathbf{x},t+\Delta t) = \frac{1}{2\pi}\int_0^{2\pi}\big(p(Q) - \varrho' c' u(Q)\cos\theta - \varrho' c' v(Q)\sin\theta\big)\,\mathrm{d}\theta$$
$$-\varrho' c'\frac{1}{2\pi}\int_0^{2\pi}\int_0^{\Delta t} S(\mathbf{x}-(\mathbf{u}'-c'\mathbf{n}(\theta))\tau, t+\Delta t-\tau,\theta)\,\mathrm{d}\tau\,\mathrm{d}\theta.$$

Now from the second and the third equation of system (4.1) we get

$$p_x = -\varrho'(u_t + u' u_x + v' u_y),$$
$$p_y = -\varrho'(v_t + u' v_x + v' v_y).$$

Hence the second term of equation (4.6) can be written as

$$(4.9)\qquad -\frac{1}{2\varrho'}\int_0^{\Delta t} p_x(P')\,\mathrm{d}\tau = \frac{1}{2}\int_0^{\Delta t}(u_\tau + u' u_x + v' u_y)\,\mathrm{d}\tau$$
$$= \int_0^{\Delta t}\nabla_{\tau,x,y}u\cdot(1,u',v')^T\,\mathrm{d}\tau.$$

Since the vector $(1,u',v')^T$ represents the direction of the bicharacteristics joining the two points P' and P, see Fig. 2, equation (4.9) implies that

$$-\frac{1}{2\varrho'}\int_0^{\Delta t} p_x(P')\,\mathrm{d}\tau = \frac{u(P)-u(P')}{2}.$$

Therefore equation (4.6) takes the form

$$(4.10)\quad u(\mathbf{x},t+\Delta t) = \frac{1}{2\pi}\int_0^{2\pi}\Big(-2\frac{p(Q)}{\varrho' c'}\cos\theta + 2u(Q)\cos^2\theta + 2v(Q)\sin\theta\cos\theta\Big)\,\mathrm{d}\theta$$
$$+\frac{1}{2\pi}\int_0^{2\pi}\int_0^{\Delta t} 2\cos\theta S(\mathbf{x}-(\mathbf{u}'-c'\mathbf{n}(\theta))\tau, t+\Delta t-\tau,\theta)\,\mathrm{d}\tau\,\mathrm{d}\theta.$$

Analogously we can show that

$$-\frac{1}{2\varrho'}\int_0^{\Delta t} p_y(P')\,\mathrm{d}\tau = \frac{v(P)-v(P')}{2}$$

and

$$(4.11)\quad v(\mathbf{x}, t+\Delta t) = \frac{1}{2\pi}\int_0^{2\pi}\Big(-2\frac{p(Q)}{\varrho' c'}\sin\theta + 2u(Q)\sin\theta\cos\theta + 2v(Q)\sin^2\theta\Big)\,\mathrm{d}\theta + \frac{1}{2\pi}\int_0^{2\pi}\int_0^{\Delta t} 2\sin\theta S(\mathbf{x}-(\mathbf{u}'-c'\mathbf{n}(\theta))\tau, t+\Delta t-\tau, \theta)\,\mathrm{d}\tau\,\mathrm{d}\theta.$$

Using [5, Lemma 2.1] and the fact that $S\cos\theta$ and $S\sin\theta$ can be neglected, because they are second order terms in time evolution, i.e. $\mathcal{O}(\Delta t^2)$, cf. [9], we can derive the following *approximate evolution operator* to the linearized Euler equations (4.1):

$$(4.12)\quad \varrho(\mathbf{x}, t+\Delta t) = \varrho(P') - \frac{p(P')}{c'^2} + \frac{1}{2\pi}\int_0^{2\pi}\Big(\frac{p(Q)}{c'^2} - 2\frac{\varrho'}{c'}u(Q)\cos\theta - 2\frac{\varrho'}{c'}v(Q)\sin\theta\Big)\,\mathrm{d}\theta + \mathcal{O}(\Delta t^2),$$

$$(4.13)\quad u(\mathbf{x}, t+\Delta t) = \frac{1}{2\pi}\int_0^{2\pi}\Big(-2\frac{p(Q)}{\varrho' c'}\cos\theta + 2u(Q)\cos^2\theta + 2v(Q)\sin\theta\cos\theta\Big)\,\mathrm{d}\theta + \mathcal{O}(\Delta t^2),$$

$$(4.14)\quad v(\mathbf{x}, t+\Delta t) = \frac{1}{2\pi}\int_0^{2\pi}\Big(-2\frac{p(Q)}{\varrho' c'}\sin\theta + 2u(Q)\sin\theta\cos\theta + 2v(Q)\sin^2\theta\Big)\,\mathrm{d}\theta + \mathcal{O}(\Delta t^2),$$

$$(4.15)\quad p(\mathbf{x}, t+\Delta t) = \frac{1}{2\pi}\int_0^{2\pi}\Big(p(Q) - 2\varrho' c' u(Q)\cos\theta - 2\varrho' c' v(Q)\sin\theta\Big)\,\mathrm{d}\theta + \mathcal{O}(\Delta t^2).$$

As we mentioned before this scheme is analogous to the EG4 scheme of the wave equation system. We call it the EG4-*Euler* scheme.

5. Numerical Examples

Example 5.1. *Rectangular waveguide*

We consider a *rectangular waveguide* with rectangular cross section of sizes a and b. The dielectric parameters are ε and μ. For transverse magnetic waves, i.e. TM modes, $H_z = 0$ and E_z satisfies the differential equation

$$(5.1)\qquad \Delta\mathbf{E} - \frac{1}{c^2}\frac{\partial^2\mathbf{E}}{\partial t^2} = 0,$$

where $c = 1/\sqrt{\varepsilon\mu}$ is the speed of wave propagation. Note that the fields $\mathbf{E}$ and $\mathbf{H}$ have in the Cartesian coordinates the form

$$\mathbf{E} = E^x\hat{\mathbf{x}} + E^y\hat{\mathbf{y}} + E^z\hat{\mathbf{z}},$$
$$\mathbf{H} = H^x\hat{\mathbf{x}} + H^y\hat{\mathbf{y}} + H^z\hat{\mathbf{z}}.$$

If the time convention $e^{i\omega t}$ is used then equation (5.1) will change to

$$\Delta \mathbf{E} + \frac{\omega^2}{c^2}\mathbf{E} = 0. \tag{5.2}$$

Further, if we assume $E^z(x,y,z) = E_0^z(x,y)e^{-\gamma z}$ then (5.2) implies that

$$\Big[\frac{\partial^2}{\partial x^2} + \frac{\partial^2}{\partial y^2} + (\gamma^2 + \frac{\omega^2}{c^2})\Big]E_0^z = 0.$$

Using the boundary conditions

$$E_0^z(0,y) = 0, \quad E_0^z(a,y) = 0, \quad E_0^z(x,0) = 0, \quad E_0^z(x,b) = 0,$$

where $0 \leqslant x \leqslant a$ and $0 \leqslant y \leqslant b$, we obtain E_0^z from the above differential equation and thus determine the electric field components E^x, E^y, E^z and the magnetic field components H^x and H^y. For example,

$$E_z(x,y,z,t) = E_0 \sin\Big(\frac{\pi}{a}x\Big)\sin\Big(\frac{\pi}{b}y\Big)\cos(\omega t - \beta z),$$

where $\gamma = i\beta = i\sqrt{\omega^2\mu\varepsilon - (m\pi/a)^2 - (n\pi/b)^2}$ for more details see [1] or [2]. If we take $\omega = c\pi\sqrt{(m/a)^2 + (n/b)^2}$, i.e. the cutoff frequency, then for the case $a = b = 1$ and $m = n = 1$ the exact solution $E_z(x,y,z,t)$ has the form

$$E^z(x,y,t) = \sin(\pi x)\sin(\pi y)\cos(\sqrt{2}\pi ct),$$

where we set $E_0 = 1$. To use the EG4 scheme denote $E_z(x,y,t)$ by $\psi(x,y,t)$ and solve the wave equation

$$\psi_{tt} = c^2(\psi_{xx} + \psi_{yy})$$

together with the initial conditions

$$\psi(x,y,0) = \sin(\pi x)\sin(\pi y), \quad \psi_t(x,y,0) = 0,$$

and the boundary conditions

$$\begin{aligned}
\psi(0,y,t) &= 0, \quad t \geqslant 0, \ 0 \leqslant y \leqslant 1,\\
\psi(1,y,t) &= 0, \quad t \geqslant 0, \ 0 \leqslant y \leqslant 1,\\
\psi(x,0,t) &= 0, \quad t \geqslant 0, \ 0 \leqslant x \leqslant 1,\\
\psi(x,1,t) &= 0, \quad t \geqslant 0, \ 0 \leqslant x \leqslant 1.
\end{aligned}$$

Defining φ, u, and v so that $\varphi = \psi_t$, $u = c\psi_x$, $v = c\psi_y$ we obtain the system

$$\begin{aligned}
\varphi_t - c(u_x + v_y) &= 0,\\
u_t - c\varphi_x &= 0,\\
v_t - c\varphi_y &= 0 \quad \text{on }]0,1[^2 \times [0,\infty[,\\
\varphi(x,y,0) &= 0,\\
u(x,y,0) &= c\pi\cos(\pi x)\sin(\pi y),\\
v(x,y,0) &= c\pi\sin(\pi x)\cos(\pi y) \quad \text{on } [0,1]^2.
\end{aligned}$$

The exact solution is

$$\begin{aligned}
\varphi &= -\sqrt{2}\pi c\sin(\pi x)\sin(\pi y)\sin(\sqrt{2}\pi ct),\\
u &= c\pi\cos(\pi x)\sin(\pi y)\cos(\sqrt{2}\pi ct),\\
v &= c\pi\sin(\pi x)\cos(\pi y)\cos(\sqrt{2}\pi ct).
\end{aligned}$$

We take $\varphi = 0$ on the boundary of Ω and extrapolate u and v there. We apply the transformations $t \to t/t_0$, $\varphi \to \varphi t_0$, $u \to ut_0$ and $v \to vt_0$ where $t_0 = \sqrt{2}\pi c$. The following two tables show the L^2-error and the experimental order of convergence (EOC), which is defined in the following way using the solutions computed on two meshes of sizes N_1, N_2:

$$\text{EOC} = \log\frac{\|\mathbf{U}_{N_1}(T) - \mathbf{U}^n_{N_1}\|}{\|\mathbf{U}_{N_2}(T) - \mathbf{U}^n_{N_2}\|} \Big/ \log\Big(\frac{N_1}{N_2}\Big).$$

Scheme	N	L^2-error-far	L^2-error-near	L^2-error
EG4	40	0.000219	0.000872	0.000899
	80	0.000091	0.000438	0.000447
	100	0.000067	0.000362	0.000368
	120	0.000054	0.000312	0.000317
	140	0.000047	0.000276	0.000280
	160	0.000039	0.000247	0.000250

Table 1. $T = 0.2$, CFL $= 0.55$, L^2-error between the discrete and the exact solutions.

In Tab. 1 the L^2-error-far represents the error in the region far from the boundary while the L^2-error-near stands for the error near the boundary.

N	$\|\varphi(T)-\varphi^n\|$	$\|u(T)-u^n\|$	$\|\mathbf{U}(T)-\mathbf{U}^n\|$	EOC
40	0.000219	0.000368	0.000564	
80	0.000091	0.000178	0.000267	1.078855
160	0.000039	0.000084	0.000125	1.094912
320	0.000019	0.000042	0.000062	1.011588
640	0.000009	0.000021	0.000031	1.000000

Table 2. EG4 scheme, $T = 0.2$, CFL $= 0.55$.

In Table 2 we measure the speed of convergence of the EG4 scheme. We see that it is approximately equal to 1, which is correct since the approximate evolution operator EG4 is of the first order in time and the shape functions are piecewise constant in space. From the tables we see that the overall L^2-error decreases as the mesh is refined. This shows that the method converges. Note that the error is dominated by an error produced due to the numerical boundary conditions, namely the extrapolation for u and v. In [7] we were able to improve this situation by using more sophisticated numerical boundary conditions. Observe again that the error in u due to the numerical boundary condition is much higher than the error in φ. For φ we can use the Dirichlet condition directly.

Example 5.2. *Divergence test*

Let $\Omega = [-1,1] \times [-1,1]$. Consider the Maxwell equations (3.1)–(3.3). Let the initial data be

$$E^z(x,y,0) = \sin\Big(\frac{\pi}{2}x\Big)\sin\Big(\frac{\pi}{2}y\Big),$$
$$H^x(x,y,0) = H^y(x,y,0) = 0 \quad \text{in } \Omega$$

and suppose that the boundary of Ω is a perfect conductor. Then using the transformations $t \to t/c$, $E^z \to \varphi$, $H^y \to u/Z_0$ and $H^x \to -v/Z_0$, these equations read

$$\frac{\partial\varphi}{\partial t} = \frac{\partial u}{\partial x} + \frac{\partial v}{\partial y}, \quad \frac{\partial u}{\partial t} = \frac{\partial\varphi}{\partial x}, \quad \frac{\partial v}{\partial t} = \frac{\partial\varphi}{\partial y}.$$

To test that the magnetic field is divergence-free remember that by the definition $\partial E^z/\partial z = 0$. Further,

$$\frac{\partial H^x}{\partial x} + \frac{\partial H^y}{\partial y} = \frac{1}{Z_0}\Big(\frac{\partial u}{\partial y} - \frac{\partial v}{\partial x}\Big).$$

Then $\nabla \cdot \mathbf{H} = 0$ can be written as $\partial u/\partial y - \partial v/\partial x = 0$, i.e. the divergence-free property is equivalent to the vanishing vorticity in the case of TM modes. In Tab. 3

we present the vorticity preservation for the EG4 scheme. We compute the discrete vorticity DV given by the formula

$$DV_{\alpha'\beta'} = \mu_x \delta_y u_{\alpha',\beta'} - \mu_y \delta_x v_{\alpha',\beta'} \quad \text{for each } \alpha', \beta' \in \mathbb{Z},$$

where we have denoted by $u_{\alpha',\beta'}$ values at vertices of square mesh cells, δ_x is used as defined before, and $\mu_x u = \frac{1}{2}\left[u(x + \frac{1}{2}h) + u(x - \frac{1}{2}h)\right]$. In Tab. 3 we show reference values for $DV_{\alpha'\beta'}$, namely, the average value (vor-aver), the minimum (vor-min) and the maximum (vor-max). The values of vor-aver demonstrate that the EG4 scheme preserves the divergence-free property in a good manner.

	100×100	200×200	400×400
vor-aver	0.00092521478	0.00029260981	0.00010088980
vor-min	−0.01221328952	−0.00948232290	−0.01140008104
vor-max	0.01221328952	0.00948232290	0.01140008104

Table 3. Preservation of zero divergence, CFL = 0.55, 100 time steps.

Example 5.3. *Linearized Euler equations problem*

In this experiment we consider linearized Euler equations

$$\mathbf{U}_t + \mathbf{A}_1(\mathbf{U}')\mathbf{U}_x + \mathbf{A}_2(\mathbf{U}')\mathbf{U}_y = 0, \quad \mathbf{x} = (x, y)^T \in]-1, 1[\times]-1, 1[, \tag{5.3}$$

where

$$\mathbf{U} := \begin{pmatrix} \varrho \\ u \\ v \\ p \end{pmatrix}, \quad \mathbf{U}' := \begin{pmatrix} 1 \\ u' \\ v' \\ 1/\gamma \end{pmatrix}, \quad \mathbf{A}_1 := \begin{pmatrix} u' & 1 & 0 & 0 \\ 0 & u' & 0 & 1 \\ 0 & 0 & u' & 0 \\ 0 & 1 & 0 & u' \end{pmatrix}, \quad \mathbf{A}_2 := \begin{pmatrix} v' & 0 & 1 & 0 \\ 0 & v' & 0 & 0 \\ 0 & 0 & v' & 1 \\ 0 & 0 & 1 & v' \end{pmatrix}.$$

Note that this system is a special case of system (4.1) with $\varrho' = c' = 1$. Here u' and v' are given constants representing the mean flow in the direction of x and y, respectively. We consider system (5.3) together with initial data containing acoustic, entropy and vorticity pulses as follows

$$\begin{aligned}
\varrho(x, y, 0) &= 2.5 \exp(-40((x - x_a)^2 + (y - y_a)^2)) \\
&\quad + 0.5 \exp(-40((x - x_b)^2 + (y - y_b)^2)), \\
u(x, y, 0) &= 0.05 \exp(-40((x - x_b)^2 + (y - y_b)^2)), \\
v(x, y, 0) &= -0.05 \exp(-40((x - x_b)^2 + (y - y_b)^2)), \\
p(x, y, 0) &= 2.5 \exp(-40((x - x_a)^2 + (y - y_a)^2)).
\end{aligned}$$

We suppose that the main flow is in the direction making a 45° angle with the x-axis and that $u' = v' = 0.5\sin(\frac{1}{4}\pi)$. Moreover, we assume that the initial location of the acoustic pulse is at $(x_a, y_a) = (-0.31, -0.31)$, whereas the entropy and vorticity is at $(x_b, y_b) = (0.39, 0.39)$. We set the CFL number ν to be 0.45 and take a mesh consisting of 100×100 cells. In Fig. 3, top-left, we compare the exact solution, the numerical solution using the first order FVEG4-Euler scheme and the Lax-Friedrichs (tensor product) scheme, which is defined by

$$\mathbf{U}^{n+1} = \frac{L_h^x \cdot L_h^y + L_h^y \cdot L_h^x}{2}\mathbf{U}^n, \tag{5.4}$$

where the operator L_h^x for the linear one dimensional system with constant coefficients

$$\mathbf{U}_t + \mathbf{A}_1\mathbf{U}_x = 0$$

is given as

$$L_h^x = \frac{\tau_h^i + \tau_{-h}^i}{2} - \frac{\Delta t}{2h}\mathbf{A}_1(\tau_h^i - \tau_{-h}^i), \quad \text{where } \tau_{\pm h}^i \mathbf{U}_{ij}^n = \mathbf{U}_{i\pm 1 j}^n.$$

The solutions are plotted along the line $y = x$ at time $T = 0.166$. In the top-right figure we show the same comparison between the second order FVEG4-Euler scheme, the Lax-Wendroff (tensor product) scheme and the exact solution. Note that the Lax-Wendroff (tensor product) scheme is defined by equation (5.7) with L_h given as

$$L_h^x = I - \left(\frac{\Delta t}{h}\right)\mathbf{A}_1\Delta_{0x} + \frac{1}{2}\left(\frac{\Delta t}{h}\right)^2\mathbf{A}_1^2\delta_x^2,$$

where $\Delta_{0x}v(x) = \frac{1}{2}[v(x+h) - v(x-h)]$, $\delta_x^2 v(x) = v(x+h) - 2v(x) + v(x-h)$. This is the symmetrical product also known as Strang splitting, see Strang [10]. In the bottom-left figure we give the comparison between the second order FVEG4-Euler scheme, the Lax-Wendroff (tensor product) scheme and the exact solution at time $T = 0.332$. In the bottom-right figure we compare the second order FVEG4-Euler scheme and the Lax-Wendroff (tensor product) scheme at time $T = 0.665$. We conclude that the acoustic part of the solution is moving faster than the entropy part and that the result using the FVEG4 first order is more accurate than that of the Lax-Friedrichs scheme. Moreover, both the FVEG4 second order and the Lax-Wendroff (tensor product) schemes give a comparable approximation of the exact solution. The difference between the schemes FVEG4 second order and the Lax-Wendroff (tensor product) as the time developed (see Fig. 3 bottom-right) is quite small for smooth solution.

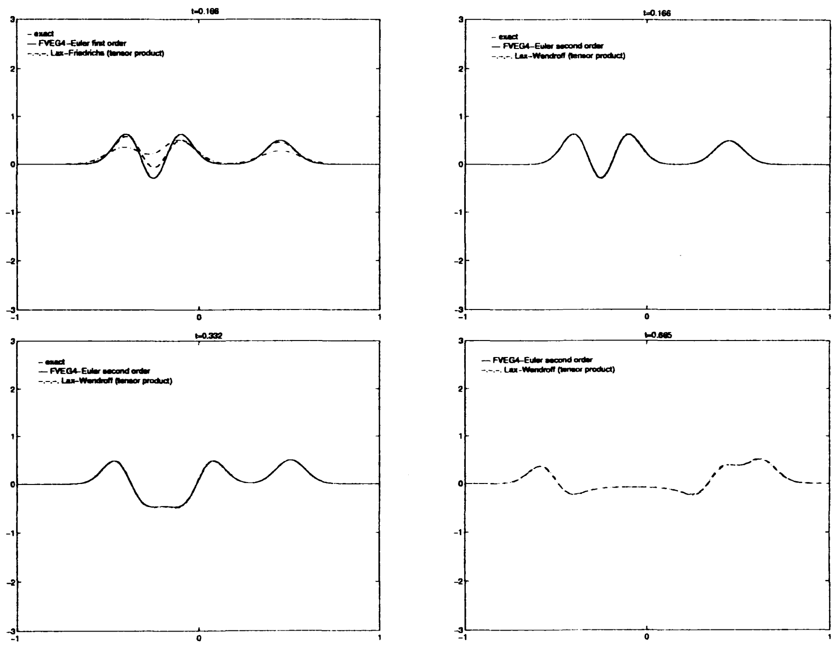

Figure 3. Density along the line $y = x$, $u' = v' = 0.5\sin(\frac{1}{4}\pi)$, CFL $= 0.45$, mesh: 100×100. Top-left: $T = 0.166$, comparison between the first order FVEG4-Euler scheme, Lax-Friedrichs (tensor product) scheme and the exact solution, top-right: $T = 0.166$, comparison between the second order FVEG4-Euler scheme, the Lax-Wendroff (tensor product) scheme and the exact solution, bottom-left: $T = 0.332$, bottom-right: $T = 0.665$, comparison between the second order FVEG4-Euler and the Lax-Wendroff (tensor product) scheme.

Conclusions.

In this paper we have derived and analyzed two approximate evolution operators (EG3, EG4) for the Maxwell equation of the electromagnetics. Both the operators are of the first order in time and are based on a general theory for multidimensional linear hyperbolic systems of the first order. As a result the numerical schemes take into account all of the infinitely many directions of wave propagation along the so-called bicharacteristic cone. Further, for the Maxwell equations the approximation of the dispersion relation was studied. It is shown that this relation is approximated with the first order error, which is correct for the piecewise constant shape functions. Moreover, it is shown that an important divergence-free property of the solution to the Maxwell equations is satisfied exactly by the approximate EG operators, i.e. EG1, EG2, EG3, EG4. In the second part of this paper we have applied the general technique of the EG-operators to the linearized Euler equations and derive a new EG4 operator for the Euler equation system. Some numerical experiments for the Maxwell equations and for the Euler equations are presented in the last section.

These experiments demonstrate good higher order as well as multi-dimensional behaviour of the FVEG schemes for linear hyperbolic systems. Generalization of the results presented in this paper to nonlinear problems can be found e.g. in [4], [6].

References

[1] *C. A. Balanis*: Advance Engineering Electromagnetics. John Wiley & Sons, New York-Chichester-Brisbane-Toronto-Singapore, 1989.

[2] *D. K. Cheng*: Field and Wave Electromagnetics. Addison-Wesley Publishing Company, second edition, 1989.

[3] *J. D. Jackson*: Classical Electrodynamics. John Wiley & Sons, third edition, New York, 1999.

[4] *M. Lukáčová-Medviďová, K. W. Morton, and G. Warnecke*: Finite volume evolution, Galerkin metods for Euler equations of gas dynamics. Internat. J. Numer. Methods Fluids *40* (2002), 425–434.

[5] *M. Lukáčová-Medviďová, K. W. Morton, and G. Warnecke*: Evolution Galerkin methods for hyperbolic systems in two space dimensions. Math. Comp. *69* (2000), 1355–1348.

[6] *M. Lukáčová-Medviďová, J. Saibertová, and G. Warnecke*: Finite volume evolution Galerkin methods for nonlinear hyperbolic systems. J. Comput. Phys. *183* (2002), 533–562.

[7] *M. Lukáčová-Medviďová, G. Warnecke, and Y. Zahaykah*: On the boundary conditions for EG-methods applied to the two-dimensional wave equation system. Z. Angew. Math. Mech. *84* (2004), 237–251.

[8] *M. Lukáčová-Medviďová, G. Warnecke, and Y. Zahaykah*: Third order finite volume evolution Galerkin (FVEG) methods for two-dimensional wave equation system. J. Numer. Math. *11* (2003), 235–251.

[9] *S. Ostkamp*: Multidimensional characteristic Galerkin schemes and evolution operators for hyperbolic systems. Math. Methods Appl. Sci. *20* (1997), 1111–1125.

[10] *G. Strang*: On the construction and comparison of difference schemes. SIAM J. Numer. Anal. *5* (1968), 506–517.

[11] *Y. Zahaykah*: Evolution Galerkin schemes and discrete boundary condition for multidimensional first order systems. PhD. thesis. Magdeburg, 2002.

Authors' addresses: *M. Lukáčová-Medviďová*, Arbeitsbereich Mathematik, Technische Universität Hamburg-Harburg, Schwarzenbergstraße 95, 21 073 Hamburg, Germany, e-mail: `lukacova@tu-harburg.de`, and Department of Mathematics, Faculty of Mechanical Engineering, University of Technology Brno, Technická 2, 616 39 Brno, Czech Republic; *J. Saibertová*, Department of Mathematics, Faculty of Mechanical Engineering, University of Technology Brno, Technická 2, 616 39 Brno, Czech Republic, e-mail: `saibertova@mat.fme.vutbr.cz`; *G. Warnecke*, Institut für Analysis und Numerik, Otto-von-Guericke-Universität Magdeburg, Universitätsplatz 2, 39 106 Magdeburg, Germany, e-mail: `Gerald.Warnecke@mathematik.uni-magdeburg.de`; *Y. Zahaykah*, Institut für Analysis und Numerik, Otto-von-Guericke-Universität Magdeburg, Universitätsplatz 2, 39 106 Magdeburg, Germany, e-mail: `Yousef.Zahaykah@mathematik.uni-magdeburg.de`.

ON EVOLUTION GALERKIN METHODS FOR THE MAXWELL AND THE LINEARIZED EULER EQUATIONS*

Mária Lukáčová-Medviďová, Hamburg and Brno, Jitka Saibertová, Brno, Gerald Warnecke, Magdeburg, and Yousef Zahaykah, Magdeburg

(Received August 19, 2002, in revised version January 29, 2003)

Abstract. The subject of the paper is the derivation and analysis of evolution Galerkin schemes for the two dimensional Maxwell and linearized Euler equations. The aim is to construct a method which takes into account better the infinitely many directions of propagation of waves. To do this the initial function is evolved using the characteristic cone and then projected onto a finite element space. We derive the divergence-free property and estimate the dispersion relation as well. We present some numerical experiments for both the Maxwell and the linearized Euler equations.

Keywords: hyperbolic systems, wave equation, evolution Galerkin schemes, Maxwell equations, linearized Euler equations, divergence-free, vorticity, dispersion

MSC 2000:

1. Introduction

Evolution Galerkin methods, EG methods, were proposed to approximate the solution of evolutionary problems of first order hyperbolic systems. Ostkamp in [9] as well as Lukáčová, Morton and Warnecke in [4], [5] derived such schemes for the approximation of the solution of the wave equation system and the Euler equations of gas dynamics in two dimensions. In [11] the approximate evolution operator for the wave equation system in three space dimensions as well as other 2D EG schemes were derived.

* This research was supported under the DFG grant No. Wa 633/6-2 of Deutsche Forschungsgemeinschaft, by the grants no. 201/00/0557 and 201/03/0570 of the Grant Agency of the Czech Republic as well as by the Volkswagen Stiftung and DAAD Agencies.

It is well-known, see [4], [5], [8], [9], that the basic tool to derive the EG schemes is the general theory of bicharacteristics of linear hyperbolic systems. This theory is used to derive the system of integral equations which is equivalent to the concerned first order system such as the Maxwell equations or the linearized Euler equations. Using quadratures, these integral equations lead to the approximate evolution operator that builds up the evolution Galerkin scheme.

Considering the Maxwell equations in free space, it is straightforward to see that the divergence of the electric field as well as of the magnetic field is zero. Numerically, in order to have an efficient Maxwell solver, this property must be preserved. Further, the dispersion relation associated with the Maxwell equations has a key role with regard to the accuracy of the numerical scheme used.

The content of this paper is as follows: in the next section we briefly derive the exact integral equations and construct evolution Galerkin schemes. In Section 3 we write down the approximate evolution operators for the Maxwell equations. Moreover, we show that these operators preserve the divergence-free property. Further, we estimate the dispersion relation for the Maxwell EG solvers that we used. In Section 4 we derive the approximate evolution operator for the linearized Euler equations. These results presented here are the basic ingredient in our extension of the method to the case of the nonlinear Euler equations, see [6]. Finally, in Section 5 we present some numerical tests for the Maxwell equations as well as the linearized Euler equations.

2. Exact integral equations and approximate evolution operators

In this section we derive exact integral equations for a general hyperbolic system in d dimensions. Typical physical examples of hyperbolic conservation laws are, e.g., the Maxwell equations and the Euler equations of gas dynamics. Using the theory of bicharacteristics one can derive the equivalent integral equations for these systems which give a basis for the EG schemes.

Let the general form of a linear hyperbolic system be given as

$$\mathbf{U}_t + \sum_{j=1}^{d} \mathbf{A}_j \mathbf{U}_{x_j} = 0, \quad \mathbf{x} = (x_1, \dots, x_d)^T \in \mathbb{R}^d \tag{2.1}$$

where the coefficient matrices $\mathbf{A}_j$, $j = 1, \dots, d$ are elements of $\mathbb{R}^{p\times p}$ and the dependent variables are $\mathbf{U} = (u_1, \dots, u_p)^T \in \mathbb{R}^p$. Let $\mathbf{A}(\mathbf{n}) = \sum_{j=1}^{d} n_j \mathbf{A}_j$ be the *pencil matrix* with $\mathbf{n} = (n_1, \dots, n_d)^T$ being a directional vector in $\mathbb{R}^d$. Then using the eigenvectors of $\mathbf{A}(\mathbf{n})$ the system (2.1) can be written in a characteristic form via the substitution $\mathbf{W} = \mathbf{R}^{-1}\mathbf{U}$, where the columns of the matrix $\mathbf{R}$ are the linearly independent right eigenvectors of $\mathbf{A}(\mathbf{n})$. Since the coefficients of the original system are constants the bicharacteristics of the resulting characteristic system are straight lines PQ_i and PP', see Fig. 1. Diagonalizing this system and integrating along the bicharacteristics leads to the system of integral equations

$$\mathbf{U}(P) = \frac{1}{|O|}\int_O \mathbf{R}(\mathbf{n})\mathbf{W}(Q(\mathbf{n}),\mathbf{n})\,\mathrm{d}O + \frac{1}{|O|}\int_O\int_0^{\Delta t} \mathbf{R}(\mathbf{n})\mathbf{S}(t+\tau,\mathbf{n})\,\mathrm{d}\tau\,\mathrm{d}O$$

where O is the unit sphere in $\mathbb{R}^d$, $|O|$ its surface measure and S is a nontrivial term which we call the source term; for more details see [8].

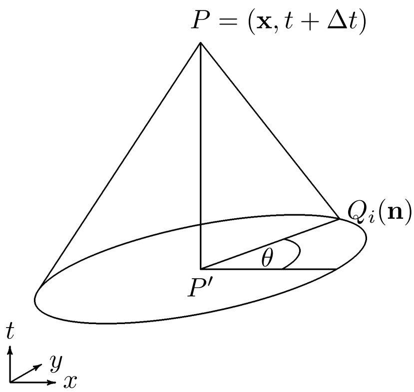

Figure 1. Bicharacteristics along the Mach cone through P and $Q_i(\mathbf{A}(\mathbf{n}))$.

Evolution Galerkin schemes

For simplicity let us consider $d = 2$. Consider $h > 0$ to be the mesh size parameter. We construct a mesh for $\mathbb{R}^2$, which consists of the square mesh cells

$$\begin{aligned}\Omega_{kl} &= \left[\left(k-\frac{1}{2}\right)h, \left(k+\frac{1}{2}\right)h\right] \times \left[\left(l-\frac{1}{2}\right)h, \left(l+\frac{1}{2}\right)h\right] \\ &= \left[x_k - \frac{h}{2}, x_k + \frac{h}{2}\right] \times \left[y_l - \frac{h}{2}, y_l + \frac{h}{2}\right],\end{aligned}$$

where $k, l \in \mathbb{Z}$. Let us denote by $H^\kappa(\mathbb{R}^2)$ the Sobolev space of distributions with derivatives up to order κ in the L^2 space, where $\kappa \in \mathbb{N}$. Consider the general hyperbolic system given by the equation (2.1). Let us denote by $E(s)\colon\ (H^\kappa(\mathbb{R}^2))^p \to (H^\kappa(\mathbb{R}^2))^p$ the exact evolution operator for the system (2.1), i.e.

$$\mathbf{U}(\cdot, t+s) = E(s)\mathbf{U}(\cdot, t). \tag{2.2}$$

We suppose that S_h^m is a finite element space consisting of piecewise polynomials of order $m \geqslant 0$ with respect to the square mesh. Assume a constant time step, i.e. $t_n = n\Delta t$. Let $\mathbf{U}^n$ be an approximation in the space S_h^m to the exact solution $\mathbf{U}(\cdot, t_n)$ at time $t_n \geqslant 0$. We consider $E_\tau\colon L^1_{\text{loc}}(\mathbb{R}^2) \to (H^\kappa(\mathbb{R}^2))^p$ to be a suitable approximate evolution operator for $E(\tau)$. In practice we will use restrictions of E_τ to the subspace S_h^m for $m \geqslant 0$. Then we can define the general class of evolution Galerkin methods.

Definition 2.1. Starting from some initial data $\mathbf{U}^0 \in S_h^m$ at time $t = 0$, an *evolution Galerkin method (EG-method)* is recursively defined by means of

$$\mathbf{U}^{n+1} = P_h E_\tau \mathbf{U}^n, \tag{2.3}$$

where P_h is the L^2-projection given by the integral averages in the following way:

$$P_h \mathbf{U}^n|_{\Omega_{kl}} = \frac{1}{|\Omega_{kl}|} \int_{\Omega_{kl}} \mathbf{U}(x, y, t_n)\,\mathrm{d}x\,\mathrm{d}y.$$

We denote by $R_h\colon S_h^m \to S_h^r$ a recovery operator, $r \geqslant m \geqslant 0$ and consider our approximate evolution operator E_τ on S_h^r. We will limit our further considerations to the case where $m = 0$ and $r = 2$. Taking piecewise constants the resulting schemes will only be of the first order, even when E_τ is approximated to a higher order. Higher order accuracy can be obtained either by taking $m > 0$, or by inserting a recovery stage R_h before the evolution step in equation (2.3) to obtain

$$\mathbf{U}^{n+1} = P_h E_\tau R_h \mathbf{U}^n. \tag{2.4}$$

This approach involves the computation of multiple integrals and becomes quite complex for higher order recoveries. To avoid this we will consider higher order evolution Galerkin schemes based on the finite volume formulation instead.

Definition 2.2. Starting from some initial data $\mathbf{U}^0 \in S_h^m$, the finite volume evolution Galerkin method (FVEG) is recursively defined by means of

$$\mathbf{U}^{n+1} = \mathbf{U}^n - \frac{1}{h} \int_0^{\Delta t} \sum_{j=1}^{2} \delta_{x_j} \mathbf{f}_j(\tilde{\mathbf{U}}^{n+\tau/\Delta t})\,\mathrm{d}\tau, \tag{2.5}$$

where $\delta_{x_j} \mathbf{f}_j(\tilde{\mathbf{U}}^{n+\tau/\Delta t})$ represents an approximation to the edge flux difference and δ_x is defined by $\delta_x = v\big(x + \frac{1}{2}h\big) - v\big(x - \frac{1}{2}h\big)$. The cell boundary value $\tilde{\mathbf{U}}^{n+\tau/\Delta t}$ is evolved using the approximate evolution operator E_τ to $t_n + \tau$ and averaged along the cell boundary, i.e.

$$\tilde{\mathbf{U}}^{n+\tau/\Delta t} = \sum_{k,l \in \mathbb{Z}} \left(\frac{1}{|\partial\Omega_{kl}|} \int_{\partial\Omega_{kl}} E_\tau R_h \mathbf{U}^n\,\mathrm{d}S \right) \chi_{kl}, \tag{2.6}$$

where χ_{kl} is the characteristic function of $\partial\Omega_{kl}$.

In this formulation a first order approximation E_τ to the exact operator $E(\tau)$ yields an overall higher order update from $\mathbf{U}^n$ to $\mathbf{U}^{n+1}$. To obtain this approximation in the discrete scheme it is only necessary to carry out a recovery stage at each level to generate a piecewise polynomial approximation $\tilde{\mathbf{U}}^n = R_h \mathbf{U}^n \in S_h^r$ from the piecewise constant $\mathbf{U}^n \in S_h^0$, to feed into the calculation of the fluxes. To construct the second order FVEG schemes, for example, we take the first order accurate approximate evolution operator and define a bilinear reconstruction R_h. Among many possible recovery schemes which can be used, we will choose a discontinuous bilinear recovery using four point averages at each vertex. It is given as

$$\begin{aligned} R_h \mathbf{U}|_{\Omega_{kl}} = \mathbf{U}_{kl} &+ \frac{x - x_k}{4h} (\Delta_{0x} \mathbf{U}_{kl+1} + 2\Delta_{0x} \mathbf{U}_{kl} + \Delta_{0x} \mathbf{U}_{kl-1}) \\ &+ \frac{y - y_l}{4h} (\Delta_{0y} \mathbf{U}_{k+1l} + 2\Delta_{0y} \mathbf{U}_{kl} + \Delta_{0y} \mathbf{U}_{k-1l}) \\ &+ \frac{(x - x_k)(y - y_l)}{h^2} \Delta_{0y} \Delta_{0x} \mathbf{U}_{kl}, \end{aligned}$$

where $\Delta_{0z} v(z) = \frac{1}{2}\big(v(z+h) - v(z-h)\big)$. Note that in the updating step (2.5) some numerical quadratures are used instead of the exact time integration. Similarly, to evaluate the intermediate value $\tilde{\mathbf{U}}^{n+\tau/\Delta t}$ in (2.6) the two dimensional integrals along the cell-interface and around the Mach cone are evaluated either exactly or by means of suitable numerical quadratures.

To close this section note that in this paper we set T to be the absolute end time of computation, i.e. $T = n\Delta t$. Further, the Courant, Friedrichs and Lewy stability number is denoted by ν and we take it to be $\nu = c\Delta t/h$ for the Maxwell equations. For the linearized Euler equation we set $\nu = \min(|u'| + c', |v'| + c')\Delta t/h$, where u', v' are the mean flows in the x and y directions respectively and c' is the local sound speed.

3. Maxwell equations

For the fundamentals of the electromagnetic theory and the Maxwell equations see Jackson [3], Balanis [1], Cheng [2]. Throughout this section we will consider the transverse magnetic (TM) modes of the electromagnetic fields only. So let us take $\mathbf{E} = E^z \hat{\mathbf{z}}$, $\mathbf{H} = H^x \hat{\mathbf{x}} + H^y \hat{\mathbf{y}}$, where $\hat{\mathbf{x}}$, $\hat{\mathbf{y}}$, $\hat{\mathbf{z}}$ are unit vectors in the direction of x, y, and z, respectively. In free space the Maxwell equations

$$\begin{aligned} \frac{\partial \mathbf{B}}{\partial t} + \nabla \times \mathbf{E} = 0, \\ -\frac{\partial \mathbf{D}}{\partial t} + \nabla \times \mathbf{H} = 0 \end{aligned}$$

are reduced to

$$\frac{\partial E^z}{\partial t} = \frac{1}{\varepsilon}\Big(\frac{\partial H^y}{\partial x} - \frac{\partial H^x}{\partial y}\Big), \tag{3.1}$$

$$\frac{\partial H^y}{\partial t} = \frac{1}{\mu}\frac{\partial E^z}{\partial x}, \tag{3.2}$$

$$\frac{\partial H^x}{\partial t} = -\frac{1}{\mu}\frac{\partial E^z}{\partial y}. \tag{3.3}$$

Here **E** denotes the electric field, **B** is the magnetic field, **D**, **H** denote the electric field density and magnetic field intensity, respectively. Further, we have $\mathbf{D} = \varepsilon\mathbf{E}$, $\mathbf{B} = \mu\mathbf{H}$, where ε is the permittivity and μ the permeability of the free space. Using the transformations $\varphi = E^z/\sqrt{\mu}$, $u = -H^y/\sqrt{\varepsilon}$, $v = H^x/\sqrt{\varepsilon}$ and taking $c = 1/\sqrt{\varepsilon\mu}$ equations (3.1)–(3.3) are reduced to the two dimensional wave equation system

$$\begin{aligned} \varphi_t + c(u_x + v_y) &= 0,\\ u_t + c\varphi_x &= 0,\\ v_t + c\varphi_y &= 0. \end{aligned} \tag{3.4}$$

Lukáčová et.al. [5] analyzed the evolution Galerkin schemes for the system (3.4). Namely, they derived the schemes EG1, EG2 and EG3. Moreover, in [11] the author derived the EG4 scheme. Note that the system (3.4) has the following property of irrotationality:

$$\frac{\mathrm{d}}{\mathrm{d}t}(u_y - v_x) = u_{ty} - v_{tx} = -c(\varphi_{xy} - \varphi_{yx}) = 0,$$

i.e. a solution with $u_y - v_x = 0$ for time $t = 0$ satisfies this equation of irrotationality for later times also. From the above we see that

$$0 = u_y - v_x = \frac{-1}{\sqrt{\varepsilon}}[(H^y)_y + (H^x)_x] = \frac{-1}{\sqrt{\varepsilon}}\nabla\cdot\mathbf{H}.$$

So the vorticity $u_y - v_x$ for the wave equation system corresponds to the divergence of the magnetic field. Using the above transformations we arrived at the following approximate evolution operators for the Maxwell equations.

Based on the EG4 scheme

$$(3.5)\quad E^z(P) = \frac{1}{2}\pi \int_0^{2\pi} [E^z(Q) + Z(2\cos\theta H^y(Q) - 2\sin\theta H^x(Q))]\, \mathrm{d}\theta + \mathcal{O}(\Delta t^2),$$

$$(3.6)\quad H^y(P) = \frac{1}{2\pi} \int_0^{2\pi} \Big[\frac{2\cos\theta E^z(Q)}{Z} + 2\cos^2\theta H^y(Q) - 2\sin\theta\cos\theta H^x(Q)\Big]\, \mathrm{d}\theta + \mathcal{O}(\Delta t^2),$$

$$(3.7)\quad H^x(P) = \frac{1}{2\pi} \int_0^{2\pi} \Big[\frac{-2\sin\theta E^z(Q)}{Z} - 2\sin\theta\cos\theta H^y(Q) + 2\sin^2\theta H^x(Q)\Big]\, \mathrm{d}\theta + \mathcal{O}(\Delta t^2).$$

Based on the EG3 scheme

$$(3.8)\qquad E^z(P) = \frac{1}{2\pi} \int_0^{2\pi} [E^z(Q) + Z(2\cos\theta H^y(Q) - 2\sin\theta H^x(Q))]\, \mathrm{d}\theta + \mathcal{O}(\Delta t^2),$$

$$(3.9)\qquad H^y(P) = \frac{1}{2}H^y(P') + \frac{1}{2\pi} \int_0^{2\pi} \Big[\frac{2\cos\theta E^z(Q)}{Z} + (3\cos^2\theta - 1)H^y(Q) - 3\sin\theta\cos\theta H^x(Q)\Big]\, \mathrm{d}\theta + \mathcal{O}(\Delta t^2),$$

$$(3.10)\qquad H^x(P) = \frac{1}{2}H^x(P') + \frac{1}{2\pi} \int_0^{2\pi} \Big[\frac{-2\sin\theta E^z(Q)}{Z} - 3\sin\theta\cos\theta H^y(Q) + (3\sin^2\theta - 1)H^x(Q)\Big]\, \mathrm{d}\theta + \mathcal{O}(\Delta t^2),$$

where $Z = \sqrt{\mu/\varepsilon}$ is the so-called impedance of free space. Taking the projection onto piecewise constant functions we obtain the evolution Galerkin schemes for the Maxwell equations. Numerical schemes based on equations (3.5)—(3.7) and (3.8)–(3.10) are called the EG4 and the EG3 methods, respectively. Note that these schemes are first order schemes. In order to have second order methods for the Maxwell equations we use the finite volume formulation as given in Definition 2.2. Assuming the periodicity of the fields in space we get the following two lemmas.

Lemma 3.1. *The approximate evolution operators for the Maxwell equations* EG3 *and* EG4 *are divergence-free.*

Proof. We prove only the case of the EG4 scheme, the EG3 scheme can be treated analogously. To this end, $\nabla\cdot\mathbf{E} = 0$ follows immediately from the assumption that $\mathbf{E} = E^z(x, y, t)\hat{\mathbf{z}}$. Now taking the derivatives with respect to y and x of the equations (3.6) and (3.7), respectively we get

(3.11)
$$\frac{\partial H^y}{\partial y}(P) = \frac{1}{2\pi}\int_0^{2\pi}\Big(\frac{2\cos\theta}{Z}\frac{\partial E^z}{\partial y}(Q) + 2\cos^2\theta\frac{\partial H^y}{\partial y}(Q) - 2\sin\theta\cos\theta\frac{\partial H^x}{\partial y}(Q)\Big)\,\mathrm{d}\theta,$$

(3.12)
$$\frac{\partial H^x}{\partial x}(P) = \frac{1}{2\pi}\int_0^{2\pi}\Big(\frac{-2\sin\theta}{Z}\frac{\partial E^z}{\partial x}(Q) - 2\sin\theta\cos\theta\frac{\partial H^y}{\partial x}(Q) + 2\sin^2\theta\frac{\partial H^x}{\partial x}(Q)\Big)\,\mathrm{d}\theta.$$

Adding equation (3.11) to the equation (3.12) we obtain

$$(3.13)\quad \frac{\partial H^x}{\partial x}(P) + \frac{\partial H^y}{\partial y}(P) = \frac{1}{2\pi}\int_0^{2\pi}\Big[\frac{2}{Z}\Big(\cos\theta\frac{\partial E^z}{\partial y}(Q) - \sin\theta\frac{\partial E^z}{\partial x}(Q)\Big) + 2\Big(\cos^2\theta\frac{\partial H^y}{\partial y}(Q) - \sin\theta\cos\theta\frac{\partial H^y}{\partial x}(Q)\Big) + 2\Big(\sin^2\theta\frac{\partial H^x}{\partial x}(Q) - \sin\theta\cos\theta\frac{\partial H^x}{\partial y}(Q)\Big)\Big]\,\mathrm{d}\theta.$$

Now the integral of the first term of equation (3.13) is zero because

$$\int_0^{2\pi}\frac{2}{Z}\Big(\cos\theta\frac{\partial E^z}{\partial y}(Q) - \sin\theta\frac{\partial E^z}{\partial x}(Q)\Big)\,\mathrm{d}\theta = \int_0^{2\pi}\frac{2}{Z}(-\sin\theta,\cos\theta)^T\cdot\nabla E^z\,\mathrm{d}\theta = \int_0^{2\pi}\frac{2}{Z}dE^z$$

and $\mathbf{E}$ is a periodic field. We use the periodicity of the magnetic field $\mathbf{H}$ and the fact that the initial data are divergence-free. Then integration by parts gives

$$(3.14)\quad \int_0^{2\pi}\Big(\cos^2\theta\frac{\partial H^y}{\partial y}(Q) - \sin\theta\cos\theta\frac{\partial H^y}{\partial x}(Q)\Big)\,\mathrm{d}\theta = \int_0^{2\pi}\cos\theta\Big(\frac{\partial H^y}{\partial y}(Q) - \sin\theta\frac{\partial H^y}{\partial x}(Q)\Big)\,\mathrm{d}\theta = \int_0^{2\pi}\cos\theta(-\sin\theta,\cos\theta)^T\cdot\nabla H^y(Q)\,\mathrm{d}\theta = \int_0^{2\pi}\cos\theta\frac{dH^y}{d\theta}(Q)\,\mathrm{d}\theta = \int_0^{2\pi}\sin\theta H^y(Q)\,\mathrm{d}\theta.$$

Analogously we have

$$(3.15)\quad \int_0^{2\pi}\Big(\sin^2\theta\frac{\partial H^x}{\partial x}(Q) - \sin\theta\cos\theta\frac{\partial H^x}{\partial y}(Q)\Big)\,\mathrm{d}\theta = \int_0^{2\pi}\cos\theta H^x(Q)\,\mathrm{d}\theta.$$

Summing equations (3.14) and (3.15) we get

$$\int_0^{2\pi}\Big(\sin^2\theta\frac{\partial H^x}{\partial x}(Q)-\sin\theta\cos\theta\frac{\partial H^y}{\partial x}(Q)+\cos^2\theta\frac{\partial H^y}{\partial y}(Q)-\sin\theta\cos\theta\frac{\partial H^x}{\partial y}(Q)\Big)\,\mathrm{d}\theta$$
$$=\int_0^{2\pi}(\cos\theta H^x(Q)+\sin\theta H^y(Q))d\theta$$
$$=\int_0^{2\pi}\mathbf{H}(Q)\cdot\mathbf{n}\,\mathrm{d}\theta=\oint\nabla\cdot\mathbf{H}(Q)\,\mathrm{d}S=0.$$

Therefore $\nabla\cdot\mathbf{H}=0$. This concludes the proof of the lemma. □

Remark 3.1. Similar results hold also for other EG operators, i.e. EG1, EG2, the operator of Ostkamp, cf. [5] for the precise formulation.

Our next aim is to approximate the dispersion relation. To this end note that a frequently used technique of characterizing the error of numerical schemes of the Maxwell equations is the Fourier analysis. Neglecting the boundary conditions, we assume that the three unknown components can be expressed in the following form:

$$\psi^n_{IJ}=\psi_0\exp\big(\mathrm{i}(\tilde{\xi}Ih+\tilde{\eta}Jh-\omega n\Delta t)\big), \tag{3.16}$$

where $\mathrm{i}=\sqrt{-1}$, h is the space increment and $\tilde{\xi}$ and $\tilde{\eta}$ are the x and y components of the numerical wave vector, respectively. In the case of the exact solution this gives

$$\psi(x,y,t)=\psi_0\exp\big(\mathrm{i}(\xi x+\eta y-\omega t)\big). \tag{3.17}$$

The numerical wave vector $\tilde{\mathbf{k}}=(\tilde{\xi},\tilde{\eta})^T$ will in general differ from the physical wave vector $\mathbf{k}=(\xi,\eta)^T$ satisfying $|\mathbf{k}|=\sqrt{\xi^2+\eta^2}=\omega/c$. This is called the dispersion relation. Here ω is the angular frequency and c is the speed of light. The difference between $\mathbf{k}$ and $\tilde{\mathbf{k}}$ gives rise to numerical phase and group velocities that depart from the analytical values. This causes numerical errors that accumulate in time. Hence the dispersion analysis is important to assess the accuracy of a numerical solution. In the next lemma we study the approximation of the dispersion relation for the EG4 method in the case of Maxwell equations.

Lemma 3.2. *For both the* EG4 *method* (3.5)–(3.7) *and the* EG3 *method* (3.8)–(3.10) *the following dispersion relation holds:*

$$\Big(\frac{\omega}{c}\Big)^2=(\tilde{\xi}^2+\tilde{\eta}^2)+\mathcal{O}(h). \tag{3.18}$$

P r o o f. We present the proof of (3.18) for the EG4 scheme, the proof for the EG3 scheme is analogous. First we write out the finite difference formulation of the EG4 scheme:

$$E^{z^{n+1}} = (1 + a_{11}(s_x^2 + s_y^2) + b_{11}s_x^2 s_y^2)E^{z^n} + Z(\nu(1 + a_{12}s_y^2)\Delta_{0x}H^{y^n} - \nu(1 + a_{13}s_x^2)\Delta_{0y}H^{x^n}), \tag{3.19}$$

$$H^{y^{n+1}} = (1 + (a_{22}s_x^2 + a'_{22}s_y^2) + b_{22}s_x^2 s_y^2)H^{y^n} + \frac{\nu}{Z}(1 + a_{21}s_y^2)\Delta_{0x}E^{z^n} - \nu^2 a_{23}\Delta_{0x}\Delta_{0y}H^{x^n}, \tag{3.20}$$

$$H^{x^{n+1}} = (1 + (a_{33}s_x^2 + a'_{33}s_y^2) + b_{33}s_x^2 s_y^2)H^{x^n} - \frac{\nu}{Z}(1 + a_{31}s_x^2)\Delta_{0y}E^{z^n} - \nu^2 a_{32}\Delta_{0x}\Delta_{0y}H^{y^n}, \tag{3.21}$$

where $\nu = c\Delta t/h$, $\Delta_{0z} = \frac{1}{2}\big(f(z+h) - f(z-h)\big)$, $s_z^2 = f(z+h) - 2f(z) + f(z-h)$ and

$$\begin{aligned}
&a_{11} = \frac{\nu}{\pi}, \quad b_{11} = \frac{\nu^2}{4\pi}, \quad a_{12} = \frac{2\nu}{3\pi}, \quad a_{13} = \frac{2\nu}{3\pi},\\
&a_{21} = \frac{2\nu}{3\pi}, \quad a_{22} = \frac{4\nu}{3\pi}, \quad a'_{22} = \frac{2\nu}{3\pi}, \quad b_{22} = \frac{\nu^2}{4\pi}, \quad a_{23} = \frac{1}{4},\\
&a_{31} = \frac{2\nu}{3\pi}, \quad a_{32} = \frac{1}{4}, \quad a_{33} = \frac{2\nu}{3\pi}, \quad a'_{33} = \frac{4\nu}{3\pi}, \quad b_{33} = \frac{\nu^2}{4\pi}.
\end{aligned}$$

Substituting from equation (3.16) into equations (3.19)–(3.21) we get

$$\begin{aligned}
-\mathrm{i}\omega\Delta t = {}& 2a_{11}(\cos(h\tilde{\xi}) - 1) + 2a_{11}(\cos(h\tilde{\eta}) - 1)\\
&+ 4b_{11}(\cos(h\tilde{\xi}) - 1)(\cos(h\tilde{\eta}) - 1)\\
&+ \mathrm{i}Z\nu\frac{H_0^y}{E_0^z}\sin(h\tilde{\xi})[1 + 2a_{12}(\cos(h\tilde{\eta}) - 1)]\\
&- \mathrm{i}Z\nu\frac{H_0^x}{E_0^z}\sin(h\tilde{\eta})[1 + 2a_{13}(\cos(h\tilde{\xi}) - 1)],
\end{aligned} \tag{3.22}$$

$$\begin{aligned}
-\mathrm{i}\omega\Delta t = {}& 2a_{22}(\cos(h\tilde{\xi}) - 1) + 2a'_{22}(\cos(h\tilde{\eta}) - 1)\\
&+ 4b_{22}(\cos(h\tilde{\xi}) - 1)(\cos(h\tilde{\eta}) - 1)\\
&+ \mathrm{i}\frac{\nu}{Z}\frac{E_0^z}{H_0^y}\sin(h\tilde{\xi})[1 + 2a_{21}(\cos(h\tilde{\eta}) - 1)]\\
&+ \nu^2 a_{23}\frac{H_0^x}{H_0^y}\sin(h\tilde{\eta})\sin(h\tilde{\xi}),
\end{aligned} \tag{3.23}$$

$$\begin{aligned}
-\mathrm{i}\omega\Delta t = {}& 2a_{33}(\cos(h\tilde{\xi}) - 1) + 2a'_{33}(\cos(h\tilde{\eta}) - 1)\\
&+ 4b_{33}(\cos(h\tilde{\xi}) - 1)(\cos(h\tilde{\eta}) - 1)
\end{aligned} \tag{3.24}$$

$$-\mathrm{i}\,\frac{\nu}{Z}\frac{E_0^z}{H_0^x}\sin(h\tilde{\eta})[1+2a_{31}(\cos(h\tilde{\xi})-1)]$$
$$+\,\nu^2 a_{32}\frac{H_0^y}{H_0^x}\sin(h\tilde{\eta})\sin(h\tilde{\xi}).$$

Now equations (3.23) and (3.24) imply, respectively, that

$$\frac{H_0^y}{E_0^z}=\frac{\frac{\nu}{Z}\sin(h\tilde{\xi})[1+2a_{21}(\cos(h\tilde{\eta})-1)]}{-\omega\Delta t+\mathrm{i}[\alpha+\nu^2 a_{23}\frac{H_0^x}{H_0^y}\sin(h\tilde{\xi})\sin(h\tilde{\eta})]},\tag{3.25}$$

$$\frac{H_0^x}{E_0^z}=\frac{\frac{\nu}{Z}\sin(h\tilde{\eta})[1+2a_{31}(\cos(h\tilde{\xi})-1)]}{\omega\Delta t-\mathrm{i}[\beta+\nu^2 a_{32}\frac{H_0^y}{H_0^x}\sin(h\tilde{\xi})\sin(h\tilde{\eta})]},\tag{3.26}$$

where

$$\alpha:=2a_{22}(\cos(h\tilde{\xi})-1)+2a'_{22}(\cos(h\tilde{\eta})-1)+4b_{22}(\cos(h\tilde{\xi})-1)(\cos(h\tilde{\eta})-1),$$
$$\beta:=2a_{33}(\cos(h\tilde{\xi})-1)+2a'_{33}(\cos(h\tilde{\eta})-1)+4b_{33}(\cos(h\tilde{\xi})-1)(\cos(h\tilde{\eta})-1).$$

Substituting equations (3.25) and (3.26) into equation (3.22) leads to

$$\omega\Delta t=\mathrm{i}\gamma-\frac{\nu^2\sin^2(h\tilde{\xi})(1+2a_{12}(\cos(h\tilde{\eta})-1))^2}{-\omega\Delta t+\mathrm{i}(\alpha+\nu^2 a_{23}\frac{H_0^x}{H_0^y}\sin(h\tilde{\xi})\sin(h\tilde{\eta}))}$$
$$-\frac{\nu^2\sin^2(h\tilde{\eta})(1+2a_{13}(\cos(h\tilde{\xi})-1))^2}{-\omega\Delta t+\mathrm{i}(\beta+\nu^2 a_{32}\frac{H_0^y}{H_0^x}}\sin(h\tilde{\xi})\sin(h\tilde{\eta})),\tag{3.27}$$

where

$$\gamma:=2a_{11}(\cos(h\tilde{\xi})-1)+2a_{11}(\cos(h\tilde{\eta})-1)+4b_{11}(\cos(h\tilde{\xi})-1)(\cos(h\tilde{\eta})-1).$$

Equation (3.27) can be written in the form

$$\begin{aligned}(\omega\Delta t-\mathrm{i}\gamma)\Big(-\omega\Delta t+\mathrm{i}\Big[\alpha+\nu^2 a_{23}\frac{H_0^x}{H_0^y}\sin(h\tilde{\xi})\sin(h\tilde{\eta})\Big]\Big)&\\ \times\Big(-\omega\Delta t+\mathrm{i}\Big[\beta+\nu^2 a_{32}\frac{H_0^y}{H_0^x}\sin(h\tilde{\xi})\sin(h\tilde{\eta})\Big]\Big)&\\ =-\nu^2\sin^2(h\tilde{\xi})[1+2a_{12}(\cos(h\tilde{\eta})-1)]^2&\\ \times\Big(-\omega\Delta t+\mathrm{i}\Big[\beta+\nu^2 a_{32}\frac{H_0^y}{H_0^x}\sin(h\tilde{\xi})\sin(h\tilde{\eta})\Big]\Big)&\\ -\nu^2\sin^2(h\tilde{\eta})[1+2a_{13}(\cos(h\tilde{\xi})-1)]^2&\\ \times\Big(-\omega\Delta t+\mathrm{i}\Big[\alpha+\nu^2 a_{23}\frac{H_0^x}{H_0^y}\sin(h\tilde{\xi})\sin(h\tilde{\eta})\Big]\Big).&\end{aligned}\tag{3.28}$$

Using the Taylor expansion we can show that γ, α and β are of order $\nu^2\mathcal{O}(h^2)$ and $\sin(hx)=hx+\mathcal{O}(h^3)$. The left- and the right-hand sides of equation (3.28) can be written as

$$
\begin{aligned}
\text{LHS} = &\Big(-\omega^2\Delta t^2 + \mathrm{i}\omega\gamma\Delta t + \mathrm{i}\omega\Delta t\Big[\alpha + \nu^2 a_{23}\frac{H_0^x}{H_0^y}\sin(h\tilde{\xi})\sin(h\tilde{\eta})\Big]\Big) \\
&+ \gamma\Big[\alpha + \nu^2 a_{23}\frac{H_0^x}{H_0^y}\sin(h\tilde{\xi})\sin(h\tilde{\eta})\Big] \\
&\times\Big(-\omega\Delta t + \mathrm{i}\Big[\beta + \nu^2 a_{32}\frac{H_0^y}{H_0^x}\sin(h\tilde{\xi})\sin(h\tilde{\eta})\Big]\Big) \\
= &\,\omega^3\Delta t^3 - \mathrm{i}\omega^2\Delta t^2\Big[\beta + \nu^2 a_{32}\frac{H_0^y}{H_0^x}\sin(h\tilde{\xi})\sin(h\tilde{\eta})\Big] - \mathrm{i}\omega^2\Delta t^2\,\gamma \\
&- \gamma\omega\Delta t\Big[\beta + \nu^2 a_{32}\frac{H_0^y}{H_0^x}\sin(h\tilde{\xi})\sin(h\tilde{\eta})\Big] \\
&- \mathrm{i}\omega^2\Delta t^2\Big[\alpha + \nu^2 a_{23}\frac{H_0^x}{H_0^y}\sin(h\tilde{\xi})\sin(h\tilde{\eta})\Big] \\
&- \omega\Delta t\Big[\alpha + \nu^2 a_{23}\frac{H_0^x}{H_0^y}\sin(h\tilde{\xi})\sin(h\tilde{\eta})\Big]\Big[\beta + \nu^2 a_{32}\frac{H_0^y}{H_0^x}\sin(h\tilde{\xi})\sin(h\tilde{\eta})\Big] \\
&- \omega\Delta t\gamma[\alpha + \nu^2 a_{23}\frac{H_0^x}{H_0^y}\sin(h\tilde{\xi})\sin(h\tilde{\eta})] \\
&+ \mathrm{i}\gamma\Big[\alpha + \nu^2 a_{23}\frac{H_0^x}{H_0^y}\sin(h\tilde{\xi})\sin(h\tilde{\eta})\Big]\Big[\beta + \nu^2 a_{32}\frac{H_0^y}{H_0^x}\sin(h\tilde{\xi})\sin(h\tilde{\eta})\Big] \\
= &\,\omega^3\Delta t^3 + \nu^2\omega\Delta t\mathcal{O}(h^3), \\
\text{RHS} = &\,\nu^2\omega\Delta t\sin^2(h\tilde{\xi}) - \nu^2\sin^2(h\tilde{\xi})\mathrm{i}\Big[\beta + \nu^2 a_{32}\frac{H_0^y}{H_0^x}\sin(h\tilde{\xi})\sin(h\tilde{\eta})\Big] \\
&+ \nu^2\omega\Delta t\sin^2(h\tilde{\xi})4a_{12}(\cos(h\tilde{\eta}) - 1) \\
&-\mathrm{i}\nu^2\sin^2(h\tilde{\xi})4a_{12}(\cos(h\tilde{\eta}) - 1)\Big[\beta + \nu^2 a_{32}\frac{H_0^y}{H_0^x}\sin(h\tilde{\xi})\sin(h\tilde{\eta})\Big] \\
&+ \nu^2\omega\Delta t\sin^2(h\tilde{\xi})4a_{12}^2(\cos(h\tilde{\eta}) - 1)^2 \\
&-\mathrm{i}\nu^2\omega\Delta t\sin^2(h\tilde{\xi})4a_{12}^2(\cos(h\tilde{\eta}) - 1)^2\Big[\beta + \nu^2 a_{32}\frac{H_0^y}{H_0^x}\sin(h\tilde{\xi})\sin(h\tilde{\eta})\Big] \\
&+ \nu^2\omega\Delta t\sin^2(h\tilde{\eta}) - \nu^2\sin^2(h\tilde{\eta})\mathrm{i}\Big[\alpha + \nu^2 a_{23}\frac{H_0^x}{H_0^y}\sin(h\tilde{\xi})\sin(h\tilde{\eta})\Big] \\
&+ \nu^2\omega\Delta t\sin^2(h\tilde{\eta})4a_{13}(\cos(h\tilde{\xi}) - 1) \\
&-\mathrm{i}\nu^2\sin^2(h\tilde{\eta})4a_{13}(\cos(h\tilde{\xi}) - 1)\Big[\alpha + \nu^2 a_{23}\frac{H_0^x}{H_0^y}\sin(h\tilde{\xi})\sin(h\tilde{\eta})\Big] \\
&+ \nu^2\omega\Delta t\sin^2(h\tilde{\eta})4a_{13}^2(\cos(h\tilde{\xi}) - 1)^2 \\
&-\mathrm{i}\nu^2\omega\Delta t\sin^2(h\tilde{\eta})4a_{13}^2(\cos(h\tilde{\xi}) - 1)^2\Big[\alpha + \nu^2 a_{23}\frac{H_0^x}{H_0^y}\sin(h\tilde{\xi})\sin(h\tilde{\eta})\Big] \\
= &\,\nu^2\omega\Delta t[\sin^2(h\tilde{\xi}) + \sin^2(h\tilde{\eta})] + \nu^2\omega\Delta t\mathcal{O}(h^3).
\end{aligned}
$$

Therefore we have

$$\omega^3 \Delta t^3 = \nu^2 \omega \Delta t [\sin^2(h\tilde{\xi}) + \sin^2(h\tilde{\eta})] + \mathcal{O}(h^3). \tag{3.29}$$

Finally, equation (3.29) leads to (3.18), which concludes the proof. □

4. Approximate evolution operators for linearized Euler equations in 2D

In this section we derive an evolution Galerkin scheme for the linearized Euler equations of gas dynamics written in primitive variables. This will be used in [6] for the fully nonlinear case. This scheme is similar to the EG4 scheme for the two-dimensional wave equation system. To define it we consider the linearized Euler equations with frozen coefficients

$$\mathbf{U}_t + \mathbf{A}_1(\mathbf{U}')\mathbf{U}_x + \mathbf{A}_2(\mathbf{U}')\mathbf{U}_y = 0, \quad \mathbf{x} = (x, y)^T \in \mathbb{R}^2, \tag{4.1}$$

where

$$\mathbf{U} := \begin{pmatrix} \varrho \\ u \\ v \\ p \end{pmatrix}, \quad \mathbf{U}' := \begin{pmatrix} \varrho' \\ u' \\ v' \\ p' \end{pmatrix}, \quad \mathbf{A}_1 := \begin{pmatrix} u' & \varrho' & 0 & 0 \\ 0 & u' & 0 & 1/\varrho' \\ 0 & 0 & u' & 0 \\ 0 & \varrho'(c')^2 & 0 & u' \end{pmatrix},$$

$$\mathbf{A}_2 := \begin{pmatrix} v' & 0 & \varrho' & 0 \\ 0 & v' & 0 & 0 \\ 0 & 0 & v' & 1/\varrho' \\ 0 & 0 & \varrho'(c')^2 & v' \end{pmatrix}.$$

Here ϱ denotes the density, u and v denote the two components of the velocity vector and p denotes the pressure. Symbols ϱ', u', v' and p' stay for the local variables at a point (x', y'), $c' = \sqrt{\gamma p'/\varrho'}$ is the local speed of the sound there and γ is the isotropic exponent ($\gamma = 1.4$ for the dry air). We use the theory presented in Section 2 to derive the integral equations that correspond to the system (4.1), see also [4], [6] for the derivation of other approximate evolution operators for the Euler equations. Thus we take the direction $\mathbf{n}(\theta) := (\cos\theta, \sin\theta)^T$ in $\mathbb{R}^2$ and define the pencil matrix to be $\mathbf{A}(\mathbf{n}) := \mathbf{A}_1 \cos\theta + \mathbf{A}_2 \sin\theta$. The eigenvectors of $\mathbf{A}(\mathbf{n})$ are

$$\begin{aligned} \lambda_1 &= u'\cos\theta + v'\sin\theta - c', \\ \lambda_2 &= \lambda_3 = u'\cos\theta + v'\sin\theta, \\ \lambda_4 &= u'\cos\theta + v'\sin\theta + c', \end{aligned}$$

and the corresponding right eigenvectors are

$$\mathbf{r}_1 = \begin{pmatrix} -\varrho'/c' \\ \cos\theta \\ \sin\theta \\ -\varrho'c' \end{pmatrix}, \quad \mathbf{r}_2 = \begin{pmatrix} 1 \\ 0 \\ 0 \\ 0 \end{pmatrix}, \quad \mathbf{r}_3 = \begin{pmatrix} 0 \\ \sin\theta \\ -\cos\theta \\ 0 \end{pmatrix}, \quad \mathbf{r}_4 = \begin{pmatrix} \varrho'/c' \\ \cos\theta \\ \sin\theta \\ \varrho'c' \end{pmatrix}.$$

Take the matrix $\mathbf{R}$ to be the matrix of the right eigenvectors. Then multiplying system (4.1) from the left by the inverse matrix

$$\mathbf{R}^{-1} = \begin{pmatrix} 0 & \cos\theta & \sin\theta & -1/(2\varrho'c') \\ 1 & 0 & 0 & -1/c'^2 \\ 0 & \sin\theta & -\cos\theta & 0 \\ 0 & \cos\theta & \sin\theta & 1/(2\varrho'c') \end{pmatrix}$$

we get the characteristic system

$$\mathbf{W}_t + \mathbf{B}_1\mathbf{W}_x + \mathbf{B}_2\mathbf{W}_y = 0, \tag{4.2}$$

where

$$\mathbf{W} = \begin{pmatrix} w_1 \\ w_2 \\ w_3 \\ w_4 \end{pmatrix} = \mathbf{R}^{-1}\mathbf{U} = \begin{pmatrix} \frac{1}{2}\big(-p/(\varrho'c') + u\cos\theta + v\sin\theta\big) \\ \varrho - p/c'^2 \\ u\cos\theta - v\sin\theta \\ \frac{1}{2}\big(p/(\varrho'c') + u\cos\theta + v\sin\theta\big) \end{pmatrix}$$

is the vector of the characteristic variables and

$$\mathbf{B}_1 = \mathbf{R}^{-1}\mathbf{A}_1\mathbf{R} = \begin{pmatrix} u' - c'\cos\theta & 0 & -\frac{1}{2}c'\sin\theta & 0 \\ 0 & u' & 0 & 0 \\ -c'\sin\theta & 0 & u' & c'\sin\theta \\ 0 & 0 & \frac{1}{2}c'\sin\theta & u' + c'\cos\theta \end{pmatrix},$$

$$\mathbf{B}_2 = \mathbf{R}^{-1}\mathbf{A}_2\mathbf{R} = \begin{pmatrix} v' - c'\sin\theta & 0 & \frac{1}{2}c'\cos\theta & 0 \\ 0 & v' & 0 & 0 \\ c'\cos\theta & 0 & v' & -c'\cos\theta \\ 0 & 0 & -\frac{1}{2}c'\cos\theta & v' + c'\sin\theta \end{pmatrix}.$$

Diagonalizing system (4.2) we end up with

$$\mathbf{W}_t + \mathbf{\Lambda}_1\mathbf{W}_x + \mathbf{\Lambda}_2\mathbf{W}_y = \mathbf{S}, \tag{4.3}$$

where

$$\mathbf{S} = \begin{pmatrix} S_1 \\ S_2 \\ S_3 \\ S_4 \end{pmatrix} = \begin{pmatrix} \frac{1}{2}c'\big(\sin\theta\partial w_3/\partial x - \cos\theta\partial w_3/\partial y\big) \\ 0 \\ c'\sin\theta\big(\partial w_1/\partial x - \partial w_4/\partial x\big) - c'\cos\theta\big(\partial w_1/\partial y - \partial w_4/\partial y\big) \\ \frac{1}{2}c'\big(-\sin\theta\partial w_3/\partial x + \cos\theta\partial w_3/\partial y\big) \end{pmatrix}$$

and

$$\boldsymbol{\Lambda}_1 = \begin{pmatrix} u' - c'\cos\theta & 0 & 0 & 0 \\ 0 & u' & 0 & 0 \\ 0 & 0 & u' & 0 \\ 0 & 0 & 0 & u' + c'\cos\theta \end{pmatrix},$$

$$\boldsymbol{\Lambda}_2 = \begin{pmatrix} v' - c'\sin\theta & 0 & 0 & 0 \\ 0 & v' & 0 & 0 \\ 0 & 0 & v' & 0 \\ 0 & 0 & 0 & v' + c'\sin\theta \end{pmatrix}.$$

Let us define the bicharacteristics $\mathbf{x}_1$, $\mathbf{x}_2$, $\mathbf{x}_3$, $\mathbf{x}_4$ corresponding to each equation of system (4.3) as

$$\begin{aligned} \frac{\mathrm{d}\mathbf{x}_1}{\mathrm{d}\tilde{t}} &:= (u' - c'\cos\theta, v' - c'\sin\theta)^T, \\ \frac{\mathrm{d}\mathbf{x}_2}{\mathrm{d}\tilde{t}} &:= (u', v')^T, \\ \frac{\mathrm{d}\mathbf{x}_3}{\mathrm{d}\tilde{t}} &:= (u', v')^T, \\ \frac{\mathrm{d}\mathbf{x}_4}{\mathrm{d}\tilde{t}} &:= (u' + c'\cos\theta, v' + c'\sin\theta)^T. \end{aligned}$$

Note that as θ varies from 0 to 2π the resulting geometry is a Mach cone shown in Fig. 2 for the supersonic case $c'^2 > u'^2 + v'^2$. Moreover, we use the initial data $\mathbf{x}_i(\mathbf{n}, t + \Delta t) = \mathbf{x}$ to solve the above ordinary differential equations backwards and

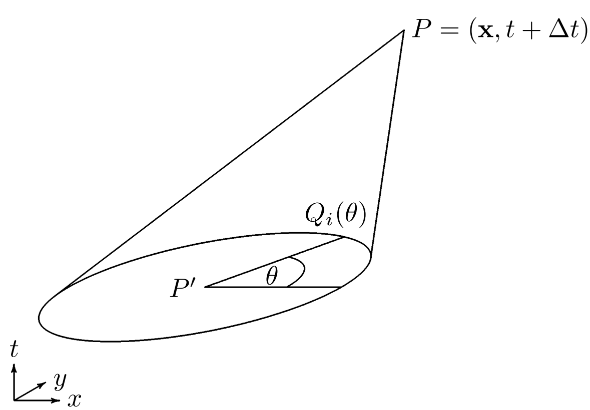

Figure 2. Bicharacteristic along the Mach cone through P and $Q_i(\theta)$, supersonic case.

get the footpoints $Q_i(\theta)$ of the bicharacteristics. The final result reads

$$
\begin{aligned}
Q_1 &= (x-(u'-c'\cos\theta)\Delta t, y-(v'-c'\sin\theta)\Delta t, t),\\
Q_2 &= Q_3 = P' = (x-u'\Delta t, y-v'\Delta t, t),\\
Q_4 &= (x-(u'+c'\cos\theta)\Delta t, y-(v'+c'\sin\theta)\Delta t, t).
\end{aligned}
$$

Now we integrate each equation of the characteristic system (4.3) along the corresponding bicharacteristic from the point $P=(x,y,t+\Delta t)$ down to the point Q where it hits the base of the Mach cone, see Fig. 2. Further, multiplying the resulting system by the matrix $\mathbf{R}$ from the left we obtain the following *integral equations*:

$$
\tag{4.4}
\begin{aligned}
\mathbf{U}_P = \frac{1}{2\pi}\int_0^{2\pi}&\begin{pmatrix} -\varrho' w_1/c' + w_2 + \varrho' w_4/c' \\ w_1\cos\theta + w_3\sin\theta + w_4\cos\theta \\ w_1\cos\theta - w_3\sin\theta + w_4\cos\theta \\ -\varrho' c' w_1 + \varrho' c' w_4 \end{pmatrix} \mathrm{d}\theta\\
&+ \frac{1}{2\pi}\int_0^{2\pi}\begin{pmatrix} -\varrho' S_1'/c' + S_2' + \varrho' S_4'/c' \\ S_1'\cos\theta + S_4'\sin\theta + S_4'\cos\theta \\ S_1'\sin\theta - S_3'\cos\theta + S_4'\sin\theta \\ -\varrho' c' S_1' + \varrho' c' S_4' \end{pmatrix} \mathrm{d}\theta,
\end{aligned}
$$

where $S_i' = \int_t^{t+\Delta t} S_i(\mathbf{x}_i(\tilde{t},\theta),\tilde{t},\theta)\,\mathrm{d}\tilde{t}$. We use the symmetry between the points Q_1 and Q_3 and the fact that the functions w_i as well as the points Q_i are 2π-periodic. Then using the notation

$$
S(\mathbf{x},t,\theta) := c'[\sin\theta^2 u_x(\mathbf{x},t,\theta) - \sin\theta\cos\theta(u_y(\mathbf{x},t,\theta)+v_x(\mathbf{x},t,\theta)) + \cos\theta^2 v_y(\mathbf{x},t,\theta)]
$$

and $Q := Q_1$ we can rewrite system (4.4) in the following form:

$$
\tag{4.5}
\begin{aligned}
\varrho(\mathbf{x},t+\Delta t) = \varrho(P') &- \frac{p(P')}{c'^2}\\
&+ \frac{1}{2\pi}\int_0^{2\pi}\Big(\frac{p(Q)}{c'^2} - \frac{\varrho'}{c'}u(Q)\cos\theta - \frac{\varrho'}{c'}v(Q)\sin\theta\Big)\,\mathrm{d}\theta\\
&- \frac{\varrho'}{c'}\frac{1}{2\pi}\int_0^{2\pi}\int_0^{\Delta t} S(\mathbf{x}-(\mathbf{u}'-c'\mathbf{n}(\theta))\tau, t+\Delta t-\tau,\theta)\,\mathrm{d}\tau\,\mathrm{d}\theta,
\end{aligned}
$$

$$
\tag{4.6}
\begin{aligned}
u(\mathbf{x},t+\Delta t) = \frac{1}{2}u(P') &- \frac{1}{2\varrho'}\int_0^{\Delta t} p_x(P')\,\mathrm{d}\tau\\
&+ \frac{1}{2\pi}\int_0^{2\pi}\Big(-\frac{p(Q)}{\varrho' c'}\cos\theta + u(Q)\cos^2\theta + v(Q)\sin\theta\cos\theta\Big)\,\mathrm{d}\theta\\
&+ \frac{1}{2\pi}\int_0^{2\pi}\int_0^{\Delta t}\cos\theta S(\mathbf{x}-(\mathbf{u}'-c'\mathbf{n}(\theta))\tau, t+\Delta t-\tau,\theta)\,\mathrm{d}\tau\,\mathrm{d}\theta,
\end{aligned}
$$

(4.7) $$v(\mathbf{x}, t+\Delta t) = \frac{1}{2}v(P') - \frac{1}{2\varrho'}\int_0^{\Delta t} p_y(P')\,\mathrm{d}\tau + \frac{1}{2\pi}\int_0^{2\pi}\Big(-\frac{p(Q)}{\varrho' c'}\sin\theta + u(Q)\sin\theta\cos\theta + v(Q)\sin^2\theta\Big)\,\mathrm{d}\theta + \frac{1}{2\pi}\int_0^{2\pi}\int_0^{\Delta t}\sin\theta S(\mathbf{x}-(\mathbf{u}'-c'\mathbf{n}(\theta))\tau, t+\Delta t-\tau, \theta)\,\mathrm{d}\tau\,\mathrm{d}\theta,$$

(4.8) $$p(\mathbf{x}, t+\Delta t) = \frac{1}{2\pi}\int_0^{2\pi}\big(p(Q) - \varrho' c' u(Q)\cos\theta - \varrho' c' v(Q)\sin\theta\big)\,\mathrm{d}\theta - \varrho' c'\frac{1}{2\pi}\int_0^{2\pi}\int_0^{\Delta t} S(\mathbf{x}-(\mathbf{u}'-c'\mathbf{n}(\theta))\tau, t+\Delta t-\tau, \theta)\,\mathrm{d}\tau\,\mathrm{d}\theta.$$

Now from the second and the third equation of system (4.1) we get

$$p_x = -\varrho'(u_t + u' u_x + v' u_y),$$
$$p_y = -\varrho'(v_t + u' v_x + v' v_y).$$

Hence the second term of equation (4.6) can be written as

(4.9) $$-\frac{1}{2\varrho'}\int_0^{\Delta t} p_x(P')\,\mathrm{d}\tau = \frac{1}{2}\int_0^{\Delta t}(u_\tau + u' u_x + v' u_y)\,\mathrm{d}\tau = \int_0^{\Delta t}\nabla_{\tau,x,y} u\cdot(1, u', v')^T\,\mathrm{d}\tau.$$

Since the vector $(1, u', v')^T$ represents the direction of the bicharacteristics joining the two points P' and P, see Fig. 2, equation (4.9) implies that

$$-\frac{1}{2\varrho'}\int_0^{\Delta t} p_x(P')\,\mathrm{d}\tau = \frac{u(P)-u(P')}{2}.$$

Therefore equation (4.6) takes the form

(4.10) $$u(\mathbf{x}, t+\Delta t) = \frac{1}{2\pi}\int_0^{2\pi}\Big(-2\frac{p(Q)}{\varrho' c'}\cos\theta + 2u(Q)\cos^2\theta + 2v(Q)\sin\theta\cos\theta\Big)\,\mathrm{d}\theta + \frac{1}{2\pi}\int_0^{2\pi}\int_0^{\Delta t} 2\cos\theta S(\mathbf{x}-(\mathbf{u}'-c'\mathbf{n}(\theta))\tau, t+\Delta t-\tau, \theta)\,\mathrm{d}\tau\,\mathrm{d}\theta.$$

Analogously we can show that

$$-\frac{1}{2\varrho'}\int_0^{\Delta t} p_y(P')\,\mathrm{d}\tau = \frac{v(P)-v(P')}{2}$$

and

$$(4.11)\quad v(\mathbf{x}, t+\Delta t) = \frac{1}{2\pi}\int_0^{2\pi}\Big(-2\frac{p(Q)}{\varrho' c'}\sin\theta + 2u(Q)\sin\theta\cos\theta + 2v(Q)\sin^2\theta\Big)\,\mathrm{d}\theta \\ + \frac{1}{2\pi}\int_0^{2\pi}\int_0^{\Delta t} 2\sin\theta S(\mathbf{x} - (\mathbf{u}' - c'\mathbf{n}(\theta))\tau, t+\Delta t-\tau, \theta)\,\mathrm{d}\tau\,\mathrm{d}\theta.$$

Using [5, Lemma 2.1] and the fact that $S\cos\theta$ and $S\sin\theta$ can be neglected, because they are second order terms in time evolution, i.e. $\mathcal{O}(\Delta t^2)$, cf. [9], we can derive the following *approximate evolution operator* to the linearized Euler equations (4.1):

$$(4.12)\quad \varrho(\mathbf{x}, t+\Delta t) = \varrho(P') - \frac{p(P')}{c'^2} + \frac{1}{2\pi}\int_0^{2\pi}\Big(\frac{p(Q)}{c'^2} - 2\frac{\varrho'}{c'}u(Q)\cos\theta \\ - 2\frac{\varrho'}{c'}v(Q)\sin\theta\Big)\,\mathrm{d}\theta + \mathcal{O}(\Delta t^2),$$

$$(4.13)\quad u(\mathbf{x}, t+\Delta t) = \frac{1}{2\pi}\int_0^{2\pi}\Big(-2\frac{p(Q)}{\varrho' c'}\cos\theta + 2u(Q)\cos^2\theta + 2v(Q)\sin\theta\cos\theta\Big)\,\mathrm{d}\theta \\ + \mathcal{O}(\Delta t^2),$$

$$(4.14)\quad v(\mathbf{x}, t+\Delta t) = \frac{1}{2\pi}\int_0^{2\pi}\Big(-2\frac{p(Q)}{\varrho' c'}\sin\theta + 2u(Q)\sin\theta\cos\theta + 2v(Q)\sin^2\theta\Big)\,\mathrm{d}\theta \\ + \mathcal{O}(\Delta t^2),$$

$$(4.15)\quad p(\mathbf{x}, t+\Delta t) = \frac{1}{2\pi}\int_0^{2\pi}\Big(p(Q) - 2\varrho' c' u(Q)\cos\theta - 2\varrho' c' v(Q)\sin\theta\Big)\,\mathrm{d}\theta \\ + \mathcal{O}(\Delta t^2).$$

As we mentioned before this scheme is analogous to the EG4 scheme of the wave equation system. We call it the EG4-*Euler* scheme.

5. Numerical Examples

Example 5.1. *Rectangular waveguide*

We consider a *rectangular waveguide* with rectangular cross section of sizes a and b. The dielectric parameters are ε and μ. For transverse magnetic waves, i.e. TM modes, $H_z = 0$ and E_z satisfies the differential equation

$$(5.1)\qquad \Delta\mathbf{E} - \frac{1}{c^2}\frac{\partial^2\mathbf{E}}{\partial t^2} = 0,$$

where $c = 1/\sqrt{\varepsilon\mu}$ is the speed of wave propagation. Note that the fields $\mathbf{E}$ and $\mathbf{H}$ have in the Cartesian coordinates the form

$$\mathbf{E} = E^x\hat{\mathbf{x}} + E^y\hat{\mathbf{y}} + E^z\hat{\mathbf{z}},$$
$$\mathbf{H} = H^x\hat{\mathbf{x}} + H^y\hat{\mathbf{y}} + H^z\hat{\mathbf{z}}.$$

If the time convention $\mathrm{e}^{\mathrm{i}\omega t}$ is used then equation (5.1) will change to

$$\Delta\mathbf{E} + \frac{\omega^2}{c^2}\mathbf{E} = 0. \tag{5.2}$$

Further, if we assume $E^z(x,y,z) = E_0^z(x,y)\mathrm{e}^{-\gamma z}$ then (5.2) implies that

$$\Big[\frac{\partial^2}{\partial x^2} + \frac{\partial^2}{\partial y^2} + (\gamma^2 + \frac{\omega^2}{c^2})\Big]E_0^z = 0.$$

Using the boundary conditions

$$E_0^z(0,y) = 0, \quad E_0^z(a,y) = 0, \quad E_0^z(x,0) = 0, \quad E_0^z(x,b) = 0,$$

where $0 \leqslant x \leqslant a$ and $0 \leqslant y \leqslant b$, we obtain E_0^z from the above differential equation and thus determine the electric field components E^x, E^y, E^z and the magnetic field components H^x and H^y. For example,

$$E_z(x,y,z,t) = E_0 \sin\Big(\frac{\pi}{a}x\Big)\sin\Big(\frac{\pi}{b}y\Big)\cos(\omega t - \beta z),$$

where $\gamma = \mathrm{i}\beta = \mathrm{i}\sqrt{\omega^2\mu\varepsilon - \big(m\pi/a\big)^2 - \big(n\pi/b\big)^2}$ for more details see [1] or [2]. If we take $\omega = c\pi\sqrt{\big(m/a\big)^2 + \big(n/b\big)^2}$, i.e. the cutoff frequency, then for the case $a = b = 1$ and $m = n = 1$ the exact solution $E_z(x,y,z,t)$ has the form

$$E^z(x,y,t) = \sin(\pi x)\sin(\pi y)\cos(\sqrt{2}\pi ct),$$

where we set $E_0 = 1$. To use the EG4 scheme denote $E_z(x,y,t)$ by $\psi(x,y,t)$ and solve the wave equation

$$\psi_{tt} = c^2(\psi_{xx} + \psi_{yy})$$

together with the initial conditions

$$\psi(x,y,0) = \sin(\pi x)\sin(\pi y), \quad \psi_t(x,y,0) = 0,$$

and the boundary conditions

$$\begin{aligned}
\psi(0,y,t) &= 0, \quad t \geqslant 0,\ 0 \leqslant y \leqslant 1,\\
\psi(1,y,t) &= 0, \quad t \geqslant 0,\ 0 \leqslant y \leqslant 1,\\
\psi(x,0,t) &= 0, \quad t \geqslant 0,\ 0 \leqslant x \leqslant 1,\\
\psi(x,1,t) &= 0, \quad t \geqslant 0,\ 0 \leqslant x \leqslant 1.
\end{aligned}$$

Defining φ, u, and v so that $\varphi = \psi_t$, $u = c\psi_x$, $v = c\psi_y$ we obtain the system

$$\begin{aligned}
\varphi_t - c(u_x + v_y) &= 0,\\
u_t - c\varphi_x &= 0,\\
v_t - c\varphi_y &= 0 \quad \text{on }]0,1[^2 \times [0,\infty[,\\
\varphi(x,y,0) &= 0,\\
u(x,y,0) &= c\pi\cos(\pi x)\sin(\pi y),\\
v(x,y,0) &= c\pi\sin(\pi x)\cos(\pi y) \quad \text{on } [0,1]^2.
\end{aligned}$$

The exact solution is

$$\begin{aligned}
\varphi &= -\sqrt{2}\pi c\sin(\pi x)\sin(\pi y)\sin(\sqrt{2}\pi ct),\\
u &= c\pi\cos(\pi x)\sin(\pi y)\cos(\sqrt{2}\pi ct),\\
v &= c\pi\sin(\pi x)\cos(\pi y)\cos(\sqrt{2}\pi ct).
\end{aligned}$$

We take $\varphi = 0$ on the boundary of Ω and extrapolate u and v there. We apply the transformations $t \to t/t_0$, $\varphi \to \varphi t_0$, $u \to ut_0$ and $v \to vt_0$ where $t_0 = \sqrt{2}\pi c$. The following two tables show the L^2-error and the experimental order of convergence (EOC), which is defined in the following way using the solutions computed on two meshes of sizes N_1, N_2:

$$\text{EOC} = \log\frac{\|\mathbf{U}_{N_1}(T) - \mathbf{U}^n_{N_1}\|}{\|\mathbf{U}_{N_2}(T) - \mathbf{U}^n_{N_2}\|} \Big/ \log\Big(\frac{N_1}{N_2}\Big).$$

Scheme	N	L^2-error-far	L^2-error-near	L^2-error
EG4	40	0.000219	0.000872	0.000899
	80	0.000091	0.000438	0.000447
	100	0.000067	0.000362	0.000368
	120	0.000054	0.000312	0.000317
	140	0.000047	0.000276	0.000280
	160	0.000039	0.000247	0.000250

Table 1. $T = 0.2$, CFL $= 0.55$, L^2-error between the discrete and the exact solutions.

In Tab. 1 the L^2-error-far represents the error in the region far from the boundary while the L^2-error-near stands for the error near the boundary.

N	$\|\varphi(T) - \varphi^n\|$	$\|u(T) - u^n\|$	$\|\mathbf{U}(T) - \mathbf{U}^n\|$	EOC
40	0.000219	0.000368	0.000564	
80	0.000091	0.000178	0.000267	1.078855
160	0.000039	0.000084	0.000125	1.094912
320	0.000019	0.000042	0.000062	1.011588
640	0.000009	0.000021	0.000031	1.000000

Table 2. EG4 scheme, $T = 0.2$, CFL $= 0.55$.

In Table 2 we measure the speed of convergence of the EG4 scheme. We see that it is approximately equal to 1, which is correct since the approximate evolution operator EG4 is of the first order in time and the shape functions are piecewise constant in space. From the tables we see that the overall L^2-error decreases as the mesh is refined. This shows that the method converges. Note that the error is dominated by an error produced due to the numerical boundary conditions, namely the extrapolation for u and v. In [7] we were able to improve this situation by using more sophisticated numerical boundary conditions. Observe again that the error in u due to the numerical boundary condition is much higher than the error in φ. For φ we can use the Dirichlet condition directly.

Example 5.2. *Divergence test*

Let $\Omega = [-1, 1] \times [-1, 1]$. Consider the Maxwell equations (3.1)–(3.3). Let the initial data be

$$\begin{aligned} E^z(x, y, 0) &= \sin\Big(\frac{\pi}{2}x\Big) \sin\Big(\frac{\pi}{2}y\Big), \\ H^x(x, y, 0) &= H^y(x, y, 0) = 0 \quad \text{in } \Omega \end{aligned}$$

and suppose that the boundary of Ω is a perfect conductor. Then using the transformations $t \to t/c$, $E^z \to \varphi$, $H^y \to u/Z_0$ and $H^x \to -v/Z_0$, these equations read

$$\frac{\partial \varphi}{\partial t} = \frac{\partial u}{\partial x} + \frac{\partial v}{\partial y}, \quad \frac{\partial u}{\partial t} = \frac{\partial \varphi}{\partial x}, \quad \frac{\partial v}{\partial t} = \frac{\partial \varphi}{\partial y}.$$

To test that the magnetic field is divergence-free remember that by the definition $\partial E^z/\partial z = 0$. Further,

$$\frac{\partial H^x}{\partial x} + \frac{\partial H^y}{\partial y} = \frac{1}{Z_0}\Big(\frac{\partial u}{\partial y} - \frac{\partial v}{\partial x}\Big).$$

Then $\nabla \cdot \mathbf{H} = 0$ can be written as $\partial u/\partial y - \partial v/\partial x = 0$, i.e. the divergence-free property is equivalent to the vanishing vorticity in the case of TM modes. In Tab. 3

we present the vorticity preservation for the EG4 scheme. We compute the discrete vorticity DV given by the formula

$$DV_{\alpha'\beta'} = \mu_x \delta_y u_{\alpha',\beta'} - \mu_y \delta_x v_{\alpha',\beta'} \quad \text{for each } \alpha', \beta' \in \mathbb{Z},$$

where we have denoted by $u_{\alpha',\beta'}$ values at vertices of square mesh cells, δ_x is used as defined before, and $\mu_x u = \frac{1}{2}\big[u\big(x + \frac{1}{2}h\big) + u\big(x - \frac{1}{2}h\big)\big]$. In Tab. 3 we show reference values for $DV_{\alpha'\beta'}$, namely, the average value (vor-aver), the minimum (vor-min) and the maximum (vor-max). The values of vor-aver demonstrate that the EG4 scheme preserves the divergence-free property in a good manner.

	100×100	200×200	400×400
vor-aver	0.00092521478	0.00029260981	0.00010088980
vor-min	−0.01221328952	−0.00948232290	−0.01140008104
vor-max	0.01221328952	0.00948232290	0.01140008104

Table 3. Preservation of zero divergence, CFL = 0.55, 100 time steps.

Example 5.3. *Linearized Euler equations problem*

In this experiment we consider linearized Euler equations

$$\mathbf{U}_t + \mathbf{A}_1(\mathbf{U}')\mathbf{U}_x + \mathbf{A}_2(\mathbf{U}')\mathbf{U}_y = 0, \quad \mathbf{x} = (x,y)^T \in \,]-1,1[\, \times \,]-1,1[, \tag{5.3}$$

where

$$\mathbf{U} := \begin{pmatrix} \varrho \\ u \\ v \\ p \end{pmatrix}, \quad \mathbf{U}' := \begin{pmatrix} 1 \\ u' \\ v' \\ 1/\gamma \end{pmatrix}, \quad \mathbf{A}_1 := \begin{pmatrix} u' & 1 & 0 & 0 \\ 0 & u' & 0 & 1 \\ 0 & 0 & u' & 0 \\ 0 & 1 & 0 & u' \end{pmatrix}, \quad \mathbf{A}_2 := \begin{pmatrix} v' & 0 & 1 & 0 \\ 0 & v' & 0 & 0 \\ 0 & 0 & v' & 1 \\ 0 & 0 & 1 & v' \end{pmatrix}.$$

Note that this system is a special case of system (4.1) with $\varrho' = c' = 1$. Here u' and v' are given constants representing the mean flow in the direction of x and y, respectively. We consider system (5.3) together with initial data containing acoustic, entropy and vorticity pulses as follows

$$\begin{aligned} \varrho(x,y,0) &= 2.5\exp(-40((x-x_a)^2 + (y-y_a)^2)) \\ &\qquad + 0.5\exp(-40((x-x_b)^2 + (y-y_b)^2)), \\ u(x,y,0) &= 0.05\exp(-40((x-x_b)^2 + (y-y_b)^2)), \\ v(x,y,0) &= -0.05\exp(-40((x-x_b)^2 + (y-y_b)^2)), \\ p(x,y,0) &= 2.5\exp(-40((x-x_a)^2 + (y-y_a)^2)). \end{aligned}$$

We suppose that the main flow is in the direction making a 45° angle with the x-axis and that $u' = v' = 0.5\sin(\frac{1}{4}\pi)$. Moreover, we assume that the initial location of the acoustic pulse is at $(x_a, y_a) = (-0.31, -0.31)$, whereas the entropy and vorticity is at $(x_b, y_b) = (0.39, 0.39)$. We set the CFL number ν to be 0.45 and take a mesh consisting of 100×100 cells. In Fig. 3, top-left, we compare the exact solution, the numerical solution using the first order FVEG4-Euler scheme and the Lax-Friedrichs (tensor product) scheme, which is defined by

$$\mathbf{U}^{n+1} = \frac{L_h^x \cdot L_h^y + L_h^y \cdot L_h^x}{2} \mathbf{U}^n, \tag{5.4}$$

where the operator L_h^x for the linear one dimensional system with constant coefficients

$$\mathbf{U}_t + \mathbf{A}_1 \mathbf{U}_x = 0$$

is given as

$$L_h^x = \frac{\tau_h^i + \tau_{-h}^i}{2} - \frac{\Delta t}{2h}\mathbf{A}_1(\tau_h^i - \tau_{-h}^i), \quad \text{where } \tau_{\pm h}^i \mathbf{U}_{ij}^n = \mathbf{U}_{i\pm 1j}^n.$$

The solutions are plotted along the line $y = x$ at time $T = 0.166$. In the top-right figure we show the same comparison between the second order FVEG4-Euler scheme, the Lax-Wendroff (tensor product) scheme and the exact solution. Note that the Lax-Wendroff (tensor product) scheme is defined by equation (5.7) with L_h given as

$$L_h^x = I - \Big(\frac{\Delta t}{h}\Big)\mathbf{A}_1\Delta_{0x} + \frac{1}{2}\Big(\frac{\Delta t}{h}\Big)^2 \mathbf{A}_1^2 \delta_x^2,$$

where $\Delta_{0x} v(x) = \frac{1}{2}[v(x+h) - v(x-h)]$, $\delta_x^2 v(x) = v(x+h) - 2v(x) + v(x-h)$. This is the symmetrical product also known as Strang splitting, see Strang [10]. In the bottom-left figure we give the comparison between the second order FVEG4-Euler scheme, the Lax-Wendroff (tensor product) scheme and the exact solution at time $T = 0.332$. In the bottom-right figure we compare the second order FVEG4-Euler scheme and the Lax-Wendroff (tensor product) scheme at time $T = 0.665$. We conclude that the acoustic part of the solution is moving faster than the entropy part and that the result using the FVEG4 first order is more accurate than that of the Lax-Friedrichs scheme. Moreover, both the FVEG4 second order and the Lax-Wendroff (tensor product) schemes give a comparable approximation of the exact solution. The difference between the schemes FVEG4 second order and the Lax-Wendroff (tensor product) as the time developed (see Fig. 3 bottom-right) is quite small for smooth solution.

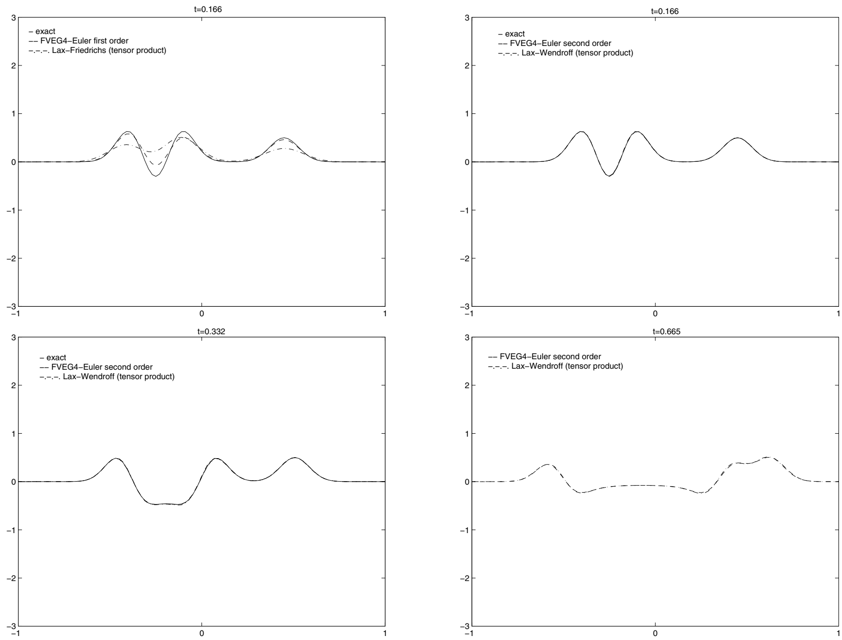

Figure 3. Density along the line $y = x$, $u' = v' = 0.5\sin(\frac{1}{4}\pi)$, CFL $= 0.45$, mesh: 100×100. Top-left: $T = 0.166$, comparison between the first order FVEG4-Euler scheme, Lax-Friedrichs (tensor product) scheme and the exact solution, top-right: $T = 0.166$, comparison between the second order FVEG4-Euler scheme, the Lax-Wendroff (tensor product) scheme and the exact solution, bottom-left: $T = 0.332$, bottom-right: $T = 0.665$, comparison between the second order FVEG4-Euler and the Lax-Wendroff (tensor product) scheme.

Conclusions.

In this paper we have derived and analyzed two approximate evolution operators (EG3, EG4) for the Maxwell equation of the electromagnetics. Both the operators are of the first order in time and are based on a general theory for multidimensional linear hyperbolic systems of the first order. As a result the numerical schemes take into account all of the infinitely many directions of wave propagation along the so-called bicharacteristic cone. Further, for the Maxwell equations the approximation of the dispersion relation was studied. It is shown that this relation is approximated with the first order error, which is correct for the piecewise constant shape functions. Moreover, it is shown that an important divergence-free property of the solution to the Maxwell equations is satisfied exactly by the approximate EG operators, i.e. EG1, EG2, EG3, EG4. In the second part of this paper we have applied the general technique of the EG-operators to the linearized Euler equations and derive a new EG4 operator for the Euler equation system. Some numerical experiments for the Maxwell equations and for the Euler equations are presented in the last section.

These experiments demonstrate good higher order as well as multi-dimensional behaviour of the FVEG schemes for linear hyperbolic systems. Generalization of the results presented in this paper to nonlinear problems can be found e.g. in [4], [6].

References

[1] *C. A. Balanis*: Advance Engineering Electromagnetics. John Wiley & Sons, New York-Chichester-Brisbane-Toronto-Singapore, 1989.

[2] *D. K. Cheng*: Field and Wave Electromagnetics. Addison-Wesley Publishing Company, second edition, 1989.

[3] *J. D. Jackson*: Classical Electrodynamics. John Wiley & Sons, third edition, New York, 1999.

[4] *M. Lukáčová-Medviďová, K. W. Morton, and G. Warnecke*: Finite volume evolution, Galerkin metods for Euler equations of gas dynamics. Internat. J. Numer. Methods Fluids *40* (2002), 425–434.

[5] *M. Lukáčová-Medviďová, K. W. Morton, and G. Warnecke*: Evolution Galerkin methods for hyperbolic systems in two space dimensions. Math. Comp. *69* (2000), 1355–1348.

[6] *M. Lukáčová-Medviďová, J. Saibertová, and G. Warnecke*: Finite volume evolution Galerkin methods for nonlinear hyperbolic systems. J. Comput. Phys. *183* (2002), 533–562.

[7] *M. Lukáčová-Medviďová, G. Warnecke, and Y. Zahaykah*: On the boundary conditions for EG-methods applied to the two-dimensional wave equation system. Z. Angew. Math. Mech. *84* (2004), 237–251.

[8] *M. Lukáčová-Medviďová, G. Warnecke, and Y. Zahaykah*: Third order finite volume evolution Galerkin (FVEG) methods for two-dimensional wave equation system. J. Numer. Math. *11* (2003), 235–251.

[9] *S. Ostkamp*: Multidimensional characteristic Galerkin schemes and evolution operators for hyperbolic systems. Math. Methods Appl. Sci. *20* (1997), 1111–1125.

[10] *G. Strang*: On the construction and comparison of difference schemes. SIAM J. Numer. Anal. *5* (1968), 506–517.

[11] *Y. Zahaykah*: Evolution Galerkin schemes and discrete boundary condition for multidimensional first order systems. PhD. thesis. Magdeburg, 2002.

Authors' addresses: *M. Lukáčová-Medviďová*, Arbeitsbereich Mathematik, Technische Universität Hamburg-Harburg, Schwarzenbergstraße 95, 21 073 Hamburg, Germany, e-mail: `lukacova@tu-harburg.de`, and Department of Mathematics, Faculty of Mechanical Engineering, University of Technology Brno, Technická 2, 616 39 Brno, Czech Republic; *J. Saibertová*, Department of Mathematics, Faculty of Mechanical Engineering, University of Technology Brno, Technická 2, 616 39 Brno, Czech Republic, e-mail: `saibertova@mat.fme.vutbr.cz`; *G. Warnecke*, Institut für Analysis und Numerik, Otto-von-Guericke-Universität Magdeburg, Universitätsplatz 2, 39 106 Magdeburg, Germany, e-mail: `Gerald.Warnecke@mathematik.uni-magdeburg.de`; *Y. Zahaykah*, Institut für Analysis und Numerik, Otto-von-Guericke-Universität Magdeburg, Universitätsplatz 2, 39 106 Magdeburg, Germany, e-mail: `Yousef.Zahaykah@mathematik.uni-magdeburg.de`.